

SSC-476

**DESIGN AND PERFORMANCE
EVALUATION METHODS FOR
CRACK ARRESTOR ENHANCED
ALUMINUM MARINE STRUCTURES**

By M. Paradkar, X. Xu, D. Hua

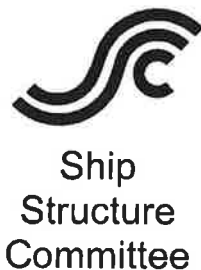


This document has been approved
for public release and sale; its
distribution is unlimited.

SHIP STRUCTURE COMMITTEE
2021

Member Agencies:

American Bureau of Shipping
Defence Research & Development Canada
Maritime Administration
Military Sealift Command
Naval Sea Systems Command
Office of Naval Research
Society of Naval Architects & Marine Engineers
Transport Canada
United States Coast Guard



Address Correspondence to:

Commandant (CG-ENG-2/SSC)
ATTN: Executive Director, SSC
US Coast Guard
2703 Martin Luther King Jr. Ave SE
Washington, DC 20593-7509
Website: <http://www.shipstructure.org>

SSC – 476
SR – 1479

13 January 2021

**DESIGN AND PERFORMANCE EVALUATION METHODS FOR CRACK ARRESTOR
ENHANCED ALUMINUM MARINE STRUCTURES**

High speed aluminum vessels pose a unique set of design challenges. These vessels are used for a variety of applications including naval craft, offshore support vessels, high speed ferries, and more. They regularly encounter high stresses, and are susceptible to rapid crack propagation. If left unchecked, cracking can cause catastrophic disaster. Crack arrest is typically achieved through targeted local use of high fracture toughness materials, mechanical means or reduction of the crack driving forces. Limited crack arrestor design procedures exist for aluminum structure precluding an optimal selection of a mechanical arrestor to prevent cracks from reaching a critical state. This report seeks to improve the existing modeling capability for crack initiation and propagation. This report also analyzes existing crack arrestor technologies to determine best practices. Armed with these best practices, high speed aluminum craft operators and designers will be able to more effectively protect the crews and cargo from hull failure marine casualties.

We thank the authors and Project Technical Committee for their dedication and research toward completing the objectives and tasks detailed throughout this paper and continuing the Ship Structure Committee's mission to enhance the safety of life at sea.

A handwritten signature in blue ink, appearing to read "R. V. Timme".

R. V. TIMME
Rear Admiral, U.S. Coast Guard
Co-Chairman, Ship Structure Committee

A handwritten signature in blue ink, appearing to read "J. M. Lloyd".

J. M. LLOYD
Rear Admiral, U.S. Navy
Co-Chairman, Ship Structure Committee

SHIP STRUCTURE COMMITTEE

RDML Richard Timme
U. S. Coast Guard Assistant Commandant
for Prevention Policy (CG-5P)
Co-Chair, Ship Structure Committee

RDML Jason Lloyd
Chief Engineer and Deputy Commander
For Naval Systems Engineering (SEA05)
Co-Chair, Ship Structure Committee

Mr. Jeffrey Lantz
Director, Commercial Regulations and Standards (CG-5PS)
U.S. Coast Guard

Mr. Gareth Burton
Vice President, Technology
American Bureau of Shipping

Mr. H. Paul Cojeen
Society of Naval Architects and Marine Engineers

Dr. John MacKay
Head, Warship Performance, DGSTCO
Defence Research & Development Canada - Atlantic

Mr. Kevin Kohlmann
Director, Office of Safety
Maritime Administration

Mr. Luc Tremblay
Executive Director, Domestic Vessel Regulatory Oversight
and Boating Safety, Transport Canada

Mr. Albert Curry
Deputy Assistant Commandant for Engineering and
Logistics (CG-4D)
U.S. Coast Guard

Mr. Eric Duncan
Group Director, Ship Integrity and Performance Engineering
(SEA 05P)
Naval Sea Systems Command

Mr. Neil Lichtenstein
Deputy Director N7x, Engineering Directorate
Military Sealift Command

Dr. Thomas Fu
Director, Ship Systems and Engineering Research Division
Office of Naval Research

SHIP STRUCTURE EXECUTIVE GROUP & SUB-COMMITTEE

UNITED STATES COAST GUARD (CVE)

CAPT Robert Compber
Mr. Jaideep Sirkar
Mr. Charles Rawson

AMERICAN BUREAU OF SHIPPING

Dr. Qing Yu
Dr. Gu Hai
Mr. Daniel LaMere
Ms. Christina Wang
Mr. Rich Delpizzo

SOCIETY OF NAVAL ARCHITECTS AND MARINE ENGINEERS

Mr. Frederick Ashcroft
Dr. Roger Basu
Dr. Robert Sielski
Dr. Paul Miller

DEFENCE RESEARCH & DEVELOPMENT CANADA ATLANTIC

Dr. Malcolm Smith
Mr. Cameron Munro
Mr. Neil Pegg

MARITIME ADMINISTRATION

Mr. Todd Hiller
Mr. Todd Ripley

TRANSPORT CANADA

Ms. Veronique Bérubé
Mr. Bashir Ahmed Golam
Ms. Tayyeba Seif

UNITED STATES COAST GUARD (FLEET)

CAPT George Leshner
Mr. Martin Hecker
Mr. Timothy McAllister
Mr. Debu Ghosh

NAVSEA/NSWCCD

Mr. David Qualley
Mr. Dean Schleicher
Dr. Pradeep Sensharma
Mr. Daniel Bruchman

MILITARY SEALIFT COMMAND

Ms. Jeannette Viernes

OFFICE OF NAVAL RESEARCH

Dr. Paul Hess

PROJECT TECHNICAL COMMITTEE

The Ship Structure Committee greatly appreciates the contributions of the individuals that volunteered their time to participate on the Project Technical Committee, listed below, and thanks them heartily. They were the subject matter expert representatives of the Ship Structure Committee to the contractor, performing technical oversight during contracting, advising the contractor in cognizant matters pertaining to the contract of which the agencies were aware, and performing technical peer review of the work in progress and upon completion.

Chair:

Mr. Charles Rawson, US Coast Guard

Members:

Chao Lin, US Maritime Administration

Jose Alberto Rosas, Class NK

Nathan Korinchak, US Navy

Gordon MacDonald, Lloyds Register

Rod Sutherland, NDI Engineering

Rong Huang (*independent*)

Dr. Pradeep Sensharma, US Naval Sea Systems Command

Dr. Robert Sielski, SNAME

Ship Structure Committee Executive Director:

LT Braden Rostad, US Coast Guard

1. Report No. SSC-476	2. Government Accession No. NTIS #PB2021-#####	3. Recipient's Catalog No.	
4. Title and Subtitle Design and Performance Evaluation Methods for Crack Arrestor Enhanced Aluminum Marine Structures		5. Report Date January 2021	
		6. Performing Organization Code N/A	
7. Author(s) Mayuresh Paradkar, Xiaolong Xu, David Hua		8. Performing Organization Report No. SSC-476	
9. Performing Organization Name and Address ABSG Consulting Inc. 1701 City Plaza Drive, Spring, Texas 77389		10. Work Unit No. (TRAIS) N/A	
		11. Contract or Grant No. GS00F026CA	
12. Sponsoring Agency Name and Address Ship Structure Committee COMMANDANT (CG-ENG-2/SSC) ATTN (ADMIN ASST/SHIP STRUCTURE COMMITTEE) US COAST GUARD 2703 MARTIN LUTHER KING JR. AVE SE MAILSTOP 7509 WASHINGTON DC 20593-7509		13. Type of Report and Period Covered Final Report	
		14. Sponsoring Agency Code CG-5P	
15. Supplementary Notes Sponsored by the Ship Structure Committee. The research completed by the above author for the Ship Structure Committee was reviewed by the Project Technical Committee for satisfactory completion of the objectives outlined in the Statement of Work developed and approved for funding by the Principal Members of the Ship Structure Committee.			
<p>16. Abstract</p> <p>Large, high-speed aluminum vessels are usually required to maintain aggressive operating limitations to prevent failure by subcritical growth of manufacturing flaws and service-induced defects. Studies have shown that the arrest of crack propagation can be achieved through either insertion of a local high fracture toughness material or reduction of the crack growth driving force. The lack of crack arrestor design procedures for aluminum structure has precluded an optimal selection of a mechanical arrestor device to stop the crack before reaching its critical state. This report aims at the development and verification of a design and performance evaluation method for crack arrestor enhanced aluminum marine structures. The objective of this project is to improve the existing modeling capability for crack initiation and propagation. This will efficiently and reliably capture the effect of a crack arrestor on the fatigue and fracture performance of a welded aluminum marine structure. Additionally, this improved capability will be used to explore an optimized design of a crack arrestor to achieve a design requirement.</p> <p>This report investigates the state of the art regarding crack propagation in aluminum, use of crack arrestor technologies to mitigate crack propagation in aluminum, and methodologies related to analysis and design of crack propagation in aluminum. The report employs advanced analysis methodologies to study crack propagation and crack arrestor performance in aluminum marine structures. The report addresses a tradeoff study to evaluate influence of various factors on performance of crack arrestors in aluminum marine structures.</p> <p>The report summarizes all phases of work highlighting all assumptions and/or gaps in the body of knowledge.</p>			
17. Key Words high-speed, aluminum, crack arrestor		18. Distribution Statement Distribution Unlimited Available from: National Technical Information Service Springfield, VA 22161	
19. Security Classif. (of this report) Unclassified	20. Security Classif. (of this page) Unclassified	21. No. of Pages 70	22. Price

CONVERSION FACTORS

(Approximate conversions to metric measures)

To convert from	to	Function	Value
LENGTH			
inches	meters	divide	39.3701
inches	millimeters	multiply by	25.4000
feet	meters	divide by	3.2808
VOLUME			
cubic feet	cubic meters	divide by	35.3149
cubic inches	cubic meters	divide by	61,024
SECTION MODULUS			
inches ² feet ²	centimeters ² meters ²	multiply by	1.9665
inches ² feet ²	centimeters ³	multiply by	196.6448
inches ⁴	centimeters ³	multiply by	16.3871
MOMENT OF INERTIA			
inches ² feet ²	centimeters ² meters	divide by	1.6684
inches ² feet ²	centimeters ⁴	multiply by	5993.73
inches ⁴	centimeters ⁴	multiply by	41.623
FORCE OR MASS			
long tons	tonne	multiply by	1.0160
long tons	kilograms	multiply by	1016.047
pounds	tonnes	divide by	2204.62
pounds	kilograms	divide by	2.2046
pounds	Newtons	multiply by	4.4482
PRESSURE OR STRESS			
pounds/inch ²	Newtons/meter ² (Pascals)	multiply by	6894.757
kilo pounds/inch ²	mega Newtons/meter ² (mega Pascals)	multiply by	6.8947
BENDING OR TORQUE			
foot tons	meter tons	divide by	3.2291
foot pounds	kilogram meters	divide by	7.23285
foot pounds	Newton meters	multiply by	1.35582
ENERGY			
foot pounds	Joules	multiply by	1.355826
STRESS INTENSITY			
kilo pound/inch ² inch ^{1/2} (ksi√in)	mega Newton MNm ^{3/2}	multiply by	1.0998
J-INTEGRAL			
kilo pound/inch	Joules/mm ²	multiply by	0.1753
kilo pound/inch	kilo Joules/m ²	multiply by	175.3



TECHNICAL REPORT
SHIP STRUCTURE COMMITTEE

**Design and Performance Evaluation Methods for Crack Arrestor
Enhanced Aluminum Marine Structures**

FINAL REPORT

January, 2021

Contract: GS00F026CA

Task Order: HSCG23-17-MSE094

Prepared by:

ABSG Consulting Inc.

1701 City Plaza Drive • Spring, Texas 77389

Tel: 281-673-2800 • www.abs-group.com

Table of Contents

List of Figures	ii
List of Tables	iii
Table of Abbreviations	iv
Acknowledgements.....	v
1 Executive Summary.....	1
2 Introduction.....	2
3 Methodology	3
4 Vessel Selection	6
4.1 Materials under Consideration.....	7
4.2 Analytical Models	7
4.3 Loading Conditions.....	9
4.4 Global FE Analysis	14
4.5 Critical Locations	17
4.6 Crack Propagation Study.....	19
4.6.1 Critical Midship Section	19
4.6.2 Critical Bow Section	24
5 Development of Crack Arrestor Models	28
5.1 Base Study Specimen without a Crack Arrestor.....	29
5.2 CRACK ARRESTOR TYPE-1 - CAH (Crack Arrest Hole)	30
5.3 CRACK ARRESTOR TYPE-2 - CAH with Interference Bolt	31
5.4 CRACK ARRESTOR TYPE-3 - CAH with Bolted Patch Plate	32
5.5 CRACK ARRESTOR TYPE-4 - CAH with Welded Patch Plate	33
5.6 CRACK ARRESTOR TYPE-5 - CAH with Interference Bolt & Welded Patch Plate	34
5.7 Performance Evaluation	36
5.7.1 Performance Evaluation Based on the Stress Intensity Factor (SIF)	36
5.7.2 Performance Evaluation Based on the Endurance to Cyclic Loading	37
6 Trade-off Study	40
6.1 Application of Crack Arrestors – Midship Section.....	40
6.2 Application of Crack Arrestors – Bow Section	43
6.3 Guidance on Selection of Crack Arrestor	46
7 Discussion and Concluding Remarks	51
8 References	52
APPENDIX A. Reference Drawings for Vessel	
APPENDIX B. Literature Review	

List of Figures

Figure 4-1: Vessel Selected for Study – High Speed Crew Boat	6
Figure 4-2: Development of 3D Analytical Models	8
Figure 4-3: Hydrodynamic Analysis – Irregular Waves	10
Figure 4-4: Structure Velocity vs. Time from the Hydrodynamic Analysis	10
Figure 4-5: CFD Analysis to obtain Hydrodynamic Pressure under Unit Velocity	11
Figure 4-6: CFD Analysis – Representing Fluid Contact with the Vessel.	11
Figure 4-7: Plot for Average Slamming Pressure per unit Area over Time	12
Figure 4-8: CFD Analysis – Pressure Contour at the time of Fluid Contact	12
Figure 4-9: Slamming Pressure Estimate for Different Loading Conditions	13
Figure 4-10: Global Model for the Midship Section	14
Figure 4-11: Vessel Stress Contours & Deformation due to Bending Moments	15
Figure 4-12: Global Model for the Bow Part.....	15
Figure 4-13: Stress Contour at the Bow Region due to Slamming Pressure	16
Figure 4-14: Local Model in the Critical Region of Side Shell & Bottom Web Frame (Bow Section)	17
Figure 4-15: Local Model in the Critical Region of Bottom Web Frame (Midship Section).....	18
Figure 4-16: Crack Tip Behavior during the Sagging and Hogging Bending Moments	18
Figure 4-17: Extracted Web Section - Refined for Crack Propagation Study – Midship Section	19
Figure 4-18: Conversion from Plate to Solid Elements and Application of Nodal displacements	20
Figure 4-19: Obtain SIF using Contour Integral Method (Model with 25mm Crack Length Shown)	20
Figure 4-20: Von Mises Stress Contour for Progressively Increasing Crack Lengths – Midship Section.....	21
Figure 4-21: Von Mises Stress Contour for Different Crack Lengths (focused at crack tip region) - Midship Section	21
Figure 4-22: SIF Range, ΔK_{eff} vs. Crack Length (mm) – Midship Section.....	23
Figure 4-23: Extracted Web Section - Refined for Crack Propagation Study– Bow Section.....	24
Figure 4-24: Von Mises Stress Contour for Progressively Increasing Crack Lengths – Bow Section.....	25
Figure 4-25: Von Mises Stress Contour for Different Crack Lengths (focused at crack tip region) – Bow Section.....	25
Figure 4-26: SIF Range, ΔK_{eff} vs. Crack Length (mm) – Bow Section	27
Figure 5-1: Different Crack Arrestors Considered for Study	28
Figure 5-2: Base Specimen without a Crack Arrestor	29
Figure 5-3: CRACK ARRESTOR TYPE-1 - CAH (Crack Arrest Hole)	30
Figure 5-4: CRACK ARRESTOR TYPE-2 - CAH (Crack Arrest Hole) with Interference Bolt.....	31
Figure 5-5: CRACK ARRESTOR TYPE-3 - CAH (Crack Arrest Hole) with Bolted Patch Plate .	32

Figure 5-6: CRACK ARRESTOR TYPE-4 - CAH (Crack Arrest Hole) with Welded Patch Plate	33
Figure 5-7: CRACK ARRESTOR TYPE-5 - CAH (Crack Arrest Hole) with Interference Bolt & Welded Patch Plate	34
Figure 5-8: Von Mises Stress Contour for Different Crack Arrestors	35
Figure 5-9: Von Mises Stress Contour Focused at the Crack Tip Region.....	35
Figure 5-10: SIF Comparison for Different Crack Arrestor Types	36
Figure 5-11: Performance under Cyclic Loading for Different Arrestors	37
Figure 5-12: Performance under Cyclic Loading for Different Arrestors (Monitoring Points)	39
Figure 6-1: Introduction of different Crack Arrestors – Midship Section.....	40
Figure 6-2: Von Mises Stress Contour Focused at the Crack Tip Region – Midship Section	41
Figure 6-3: Von Mises Stress Contour Focused at the Crack Tip Region– Midship Section	41
Figure 6-4: SIF Comparison for Different Crack Arrestor Types – Midship Section.....	42
Figure 6-5: Introduction of different Crack Arrestors – Bow Section	43
Figure 6-6: Von Mises Stress Contour for Different Crack Arrestors – Bow Section.....	44
Figure 6-7: Von Mises Stress Contour Focused at the Crack Tip Region – Bow Section.....	44
Figure 6-8: SIF Comparison for Different Crack Arrestor Types – Bow Section	45
Figure 6-9: CRACK ARRESTOR TYPE-3A - CAH (Crack Arrest Hole) with Single Row Bolted Patch Plate	47
Figure 6-10: CRACK ARRESTOR TYPE-3B - CAH (Crack Arrest Hole) with Double Row Bolted Patch Plate	48
Figure 6-11: CRACK ARRESTOR TYPE-4A - CAH (Crack Arrest Hole) with Long Bolted Patch and Weld-up CAH & Crack Line under Patch	49

List of Tables

Table 4-1 : Vessel Particulars	7
Table 4-2 : Loading Particulars	9
Table 4-3 : Wave Induced Bending Moments.....	9
Table 4-4 : SIF Output for Different Crack Lengths with Contour Integral Method – Midship	22
Table 4-5 : SIF Output for Different Crack Lengths with Contour Integral Method – Bow.....	26
Table 5-1 : Material Properties	29
Table 5-2 : Statistics of Crack Growth Rate for Different Crack Arrestor Types	39

Table of Abbreviations

Abbreviation ¹⁾	Description
ABS	American Bureau of Shipping
ABSG	ABS Group Consulting Inc.
ANSYS	Analytical Systems - FEA Software
ASTM	American Society of Testing & Materials
BHD	Bulkhead
BM	Bending Moment
CAH	Crack Arrest Hole
CFD	Computational Fluid Dynamics
DNV	Det Norske Veritas
FCG	Fatigue Crack Growth
FEA	Finite Element Analysis
FEMAP	Finite Element Modeling & Post processing - FEA Software
GOM	Gulf of Mexico
IMO	International Maritime Organization
LWL	Load Waterline Length
MAPTIS	Materials and Processes Technical Information System
NASA	National Aeronautics and Space Administration
NASTRAN	<u>NASA Structure Analysis Solver</u>
NAVSEA	Naval Sea Systems Command
NSWC	Naval Surface Warfare Center
SIF	Stress Intensity Factor
SNAME	Society of Naval Architect and Marine Engineers
SSC	Ship Structure Committee
USCG	United States Coast Guard
XFEM	Extended Finite Element Method

¹⁾ Arranged in alphabetical order.

Acknowledgements

This study has been funded by the Ship Structure Committee (SSC).

The authors would like to thank all the members of the Project Technical Committee (PTC) for their valuable technical feedback and suggestions throughout the project which is gratefully appreciated.

The authors would also like to especially acknowledge the support from the SSC Coordinator & Executive Director - LT Jonathan Duffett, PTC Chair Naval Architecture Division - Charles Rawson, and ABSG Project Coordinator - Joseph Myers for extending their immense support throughout the project.

1 Executive Summary

ABS Consulting Inc. (ABSG) has been tasked by the SSC through the USCG to develop and verify a design and performance evaluation method for crack arrestor enhanced aluminum marine structures.

The objective of this project is to improve the existing modeling capability for crack initiation and propagation. This will efficiently and reliably capture the effect of a crack arrestor on the fatigue and fracture performance of a welded aluminum marine structure. Additionally, this improved capability will be used to explore an optimized design of a crack arrestor to achieve a design requirement.

In order to meet the project objectives, following five (5) distinct tasks were performed:

- *Task 1: Literature Review*
- *Task 2: Modeling and Prediction of Crack Initiation and Growth*
- *Task 3: Perform a Tradeoff Study*
- *Task 4: Modeling Verification & Validation*
- *Task 5: Technical Report Writing*

This report summarizes the work performed under the above-mentioned tasks, the results obtained, and provides a detailed explanation of the methodology used to meet the project objectives.

The subject report is a consolidated summary of all the previous progress reports issued during the course of this project.

2 Introduction

Large, high-speed aluminum vessels are usually required to maintain aggressive operating limitations to prevent failure by subcritical growth of manufacturing flaws and service-induced defects. Studies have shown that the arrest of crack propagation can be achieved through either insertion of a local high fracture toughness material or reduction of the crack growth driving force. The lack of crack arrestor design procedures for aluminum structure has precluded an optimal selection of a mechanical arrestor device to stop the crack before reaching its critical state.

ABS Consulting Inc. (ABSG) has been tasked by the SSC through the USCG to develop and verify a design and performance evaluation method for crack arrestor enhanced aluminum marine structures.

The objective of this project is to improve the existing modeling capability for crack initiation and propagation. This will efficiently and reliably capture the effect of a crack arrestor on the fatigue and fracture performance of a welded aluminum marine structure. Additionally, this improved capability will be used to explore an optimized design of a crack arrestor to achieve a design requirement.

The main objectives of the subject project are as follows:

- Investigate the state of the art with regard to crack propagation in aluminum, use of crack arrestor technologies to mitigate crack propagation in aluminum, and methodologies related to analysis and design of crack propagation in aluminum.
- Employ advanced analysis methodologies to study crack propagation and crack arrestor performance in aluminum marine structures.
- Conduct tradeoff study to evaluate influence of various factors on performance of crack arrestors in aluminum marine structures.
- Verify and validate modeling and analytical techniques against known performance (e.g. testing and other relevant published data) to affirm adequacy of modeling approaches.
- Prepare a comprehensive technical report summarizing all phases of work highlighting all assumptions and/or gaps in the body of knowledge.

3 Methodology

In order to accomplish the project objectives, the efforts were divided into following five (5) distinct tasks and the method of execution of these tasks are discussed in detail below:

➤ Task 1: Literature Review

As part of the literature review, ABSG conducted an extensive search and collected literature from various sources to identify the state-of-the-art techniques and issues associated with aluminum materials used in marine structures; the fatigue and fracture properties of welded aluminum structures; crack initiation and propagation; and current design practice of crack arrestors.

Based on the collected documents, ABSG reviewed the theoretical assumptions, analytical solutions, and numerical simulations of these problems. In addition, ABSG also collected and reviewed the fatigue and fracture properties of these alloys and available test data as part of the literature review, so that the test data could be used for validation of the work. The following sources were utilized for conducting the search and collecting the relevant information:

- *Peer reviewed technical papers from Society of Naval Architect and Marine Engineers (SNAME), such as Journal of Ship Research; Marine Technology; Section papers; Symposia papers; Technical and Research reports and bulletins; and Transactions*
- *NASA MAPTIS database, which includes material properties and test data for a variety of aluminum alloys*
- *ASTM*
- *IMO Codes and guidance documents*
- *Ship Structure Committee publications, including SSC-448, SSC-452, and SSC-464*
- *ABS Rules and Guidelines*
- *DNV Rules and Recommended Practices*
- *Other international conference papers*
- *Test laboratory results from NAVSEA, NSWG, etc., related to aluminum marine structures such as strength/strain tests, fatigue and crack initiation tests, crack propagation tests, and crack arrestors effectiveness*

A list of the articles that ABSG has collected and reviewed as part of this task -1, Literature Review, are summarized in **Appendix – B** of this report.

➤ Task 2: Modeling and Prediction of Crack Initiation and Growth

The primary objective of the modeling effort was to analyze a ship with an assumed propagating crack and investigate the crack tip propagation in aluminum alloys under loading. Due to the empirical nature of ship design and lack of test data regarding crack arrest method performance, ABSG investigated the performance of various methods using finite element analysis (FEA) coupled with linear elastic fracture mechanics principles. As there is limited data that may complicate this approach being used, ABSG also considered employing the Local FE models developed in the approach described

below and potentially expanding the modeling effort to include additional parameters such as extrinsic and intrinsic stress ratios, amplitude loading variance, crack directionality, crack tip closure, and effects of residual stress. Based on the literature review, the modeling approach was adjusted to account for potential impacts from the parameters above.

➤ **Task 3: Perform a Tradeoff Study**

Several crack arrestor methods and practices, considered to not change the original design details, for aluminum ship structures have been developed in the industry. They can be summarized as follows:

- Gouging, Grinding and welding
- Drilling a hole at the crack tips
- Interference bolts to apply compressive stress
- Welded inserts
- Bolted doubler plates
- Composite patched plates

ABSG studied five (5) different type of crack arrestors that are discussed in detail under Section 5 of this report. The selection of these crack arrestors was based on the practicability and the ease of execution in field without having the structure undergo complicated repair procedures. The development of the crack arrestors was based on the following goals:

- Simplicity of design & application
- Reduction in the crack driving force to improve local fracture toughness.
- Improvement in the fatigue performance
- Extrinsic approach to arrest the crack without changing the metallurgical properties of the parent material
- Cost effectiveness
- Minimum downtime in operations due to repairs
- Minimum or No Hot Work
- Minimum or No special tooling requirement for skilled labor executing the repairs

The same local model from the previous task was modified to simulate different types of crack arrestors that could be easily incorporated into the Local FE model. During this task, ABSG investigated the influence of various parameters in the model to quantify the influence of the various arrestor methods on the crack growth. The tradeoff analysis was performed such that all methods could be quantifiably compared.

➤ **Task 4: Modeling Verification & Validation**

With the analytic models and techniques developed from Tasks 1 through 3, ABSG validated the models and techniques using the limited laboratory test results from the literature review task. The purpose of the validation or verification was to evaluate the accuracy and efficiency of the models and their solutions for crack growth simulations with various arrestors as defined during Task 3.

ABSG found limited data crack arrestor performance in aluminum ships, thus a key aspect of this task was to establish proper crack growth properties in the Local FE model without a crack arrestor.

During the verification and validation phase, ABSG verified the effect of crack arrestors considering stress intensity and stress directions that could reduce crack growth, could increase of the local fracture toughness, as well as a combination of both. As part of the validation process, ABSG considered the practicality and feasibility of implementing these arrestors and their impact on current design specification and cost of materials, fabrication, and installation, in addition to potentially introducing crack initiation and residual stress.

➤ **Task 5: Technical Report**

The last task of the project was to develop a comprehensive report that summarizes the work performed under the above-mentioned tasks, the results obtained, and a detailed explanation of the methodology used to meet the project objectives.

This subject report is a consolidated summary of all the previous progress reports issued during the course of this project.

4 Vessel Selection

For the project study purpose, a High-Speed Aluminum Crew / Patrol Boat was selected that is most commonly operated in the field (or GOM waters). The general arrangement of the selected vessel is shown in Figure 4-1. The higher resolution GA drawings are attached in Appendix-A of this report for reference purposes.

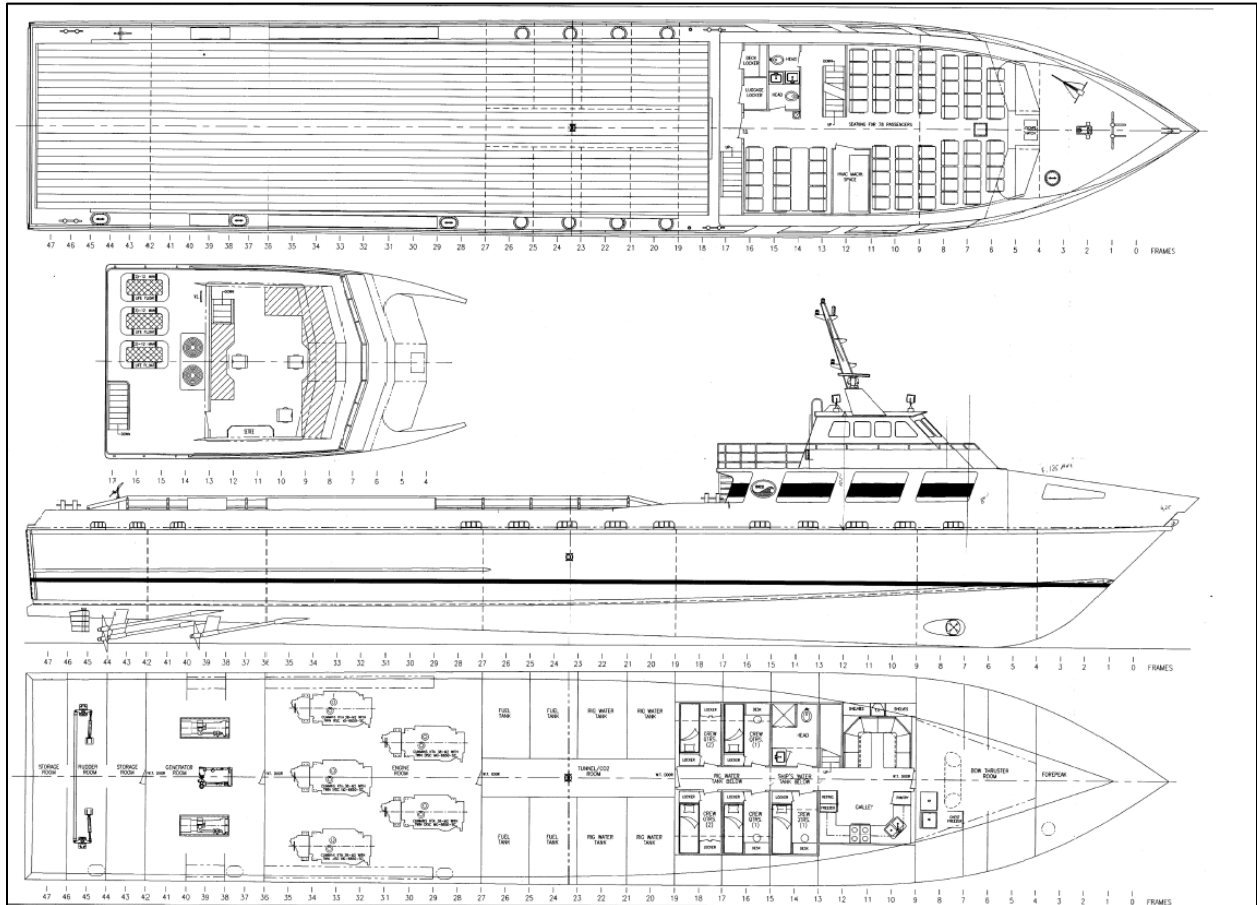


Figure 4-1: Vessel Selected for Study – High Speed Crew Boat

Table 4-1 below represents the vessel particulars considered for global analysis (principal hull dimensions and the capacities).

Table 4-1 : Vessel Particulars

Principal Hull Dimensions	Capacities
<ul style="list-style-type: none"> - Length Over All = 150' - Length on Waterline = 141.25' - Breadth = 28' - Mid-ship Depth = 13.5' - Frame Spacing = 38" Fr.36-Fwd, 31" Fr.36-Aft 	<ul style="list-style-type: none"> - Fuel = 24,000 Gallons - Rig Water = 31,500 Gallons - Ship's Water = 1500 Gallons - Deck Cargo = 250 Lt - Passengers = 73 - Crew = 7

4.1 Materials under Consideration

The subject vessel's structural members and shell plating consisted of two (2) type material as follows:

- **PLATING:** 5086 H-116 ALLOY ALUMINUM
- **EXTRUSIONS:** 6061-T6 ALLOY ALUMINUM

In this study, the identified critical locations were pertaining to the structural components with 5086 H-116 alloy aluminum and they are studied in later sections of the report.

4.2 Analytical Models

A full-scale 3D surface model was developed in FEMAP software that was used for various analytical studies during the course of the project. However, the primary focus was given to the hull structural portion of the vessel, further selecting two (2) locations of interest, i.e. the midship section being typically subjected to maximum bending moments and bow section which is subjected to maximum slamming pressure. The 3D analytical models are shown in Figure 4-2 below.

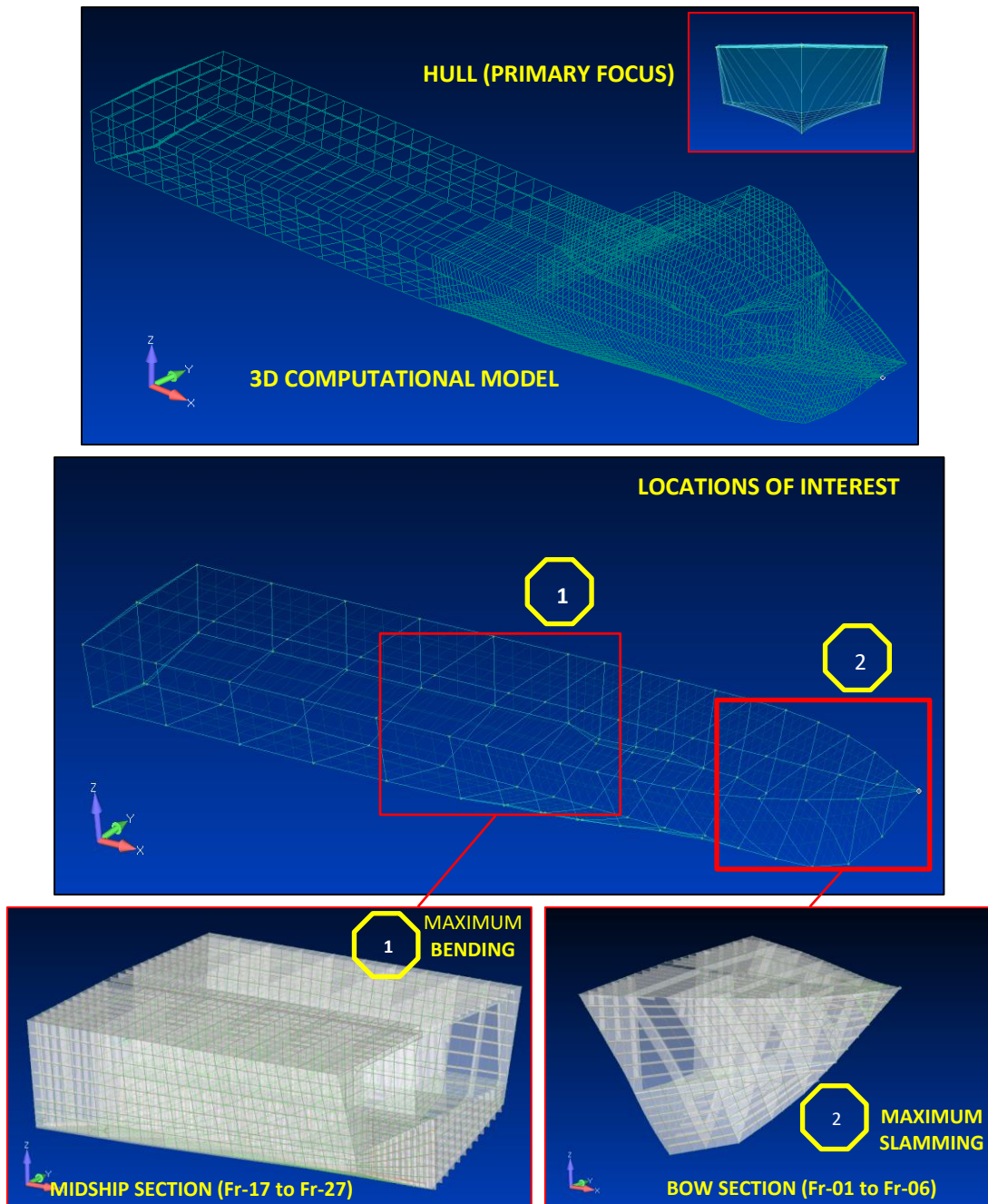


Figure 4-2: Development of 3D Analytical Models

4.3 Loading Conditions

In order to simulate a real vessel performance and identify the critical structural locations prone to fatigue damage, a global analysis was performed considering three (3) operating loading conditions as presented in Table 4-2 below:

Table 4-2 : Loading Particulars

Loading Condition	LWL	Baseline Draft	Midship Draft	Displacement		Speed	Wave Ht.	Trim (by stern)
	ft.	ft.	ft.	lbs.	LT	Kts.	ft.	deg.
LIGHT LOAD	139.000	6	4.42	450000	201	28	11	4
MEDIUM LOAD	140.420	7.25	5.67	698000	312	24	11	4
FULL LOAD	141.800	8.5	7.05	952000	425	20	11	4

The midship section under consideration was subjected to the maximum wave induced bending moments and is represented in Table 4-3 below:

Table 4-3 : Wave Induced Bending Moments

Location (Mid-ship Section)	Total BM	
	Ltf-ft	N-m
HOGGING BM	5891.59	17892950.17
SAGGING BM	4119.78	12511905.66

A hydrodynamic analysis was performed using ANSYS AQWA module, under the loading conditions and corresponding vessel forward speed as listed in Table 4-2, for three (3) distinct wave directions as shown in Figure 4-3. The wave data corresponding to Sea-State 5 (i.e. Significant Wave Height of $H_s = 11\text{ft}$ & Wave Period $T_p = 9.5\text{s}$) was considered for the analysis purpose.

Figure 4-4 below is a representative time history plot of structures velocity with the vessel moving forward under light loading conditions and waves acting in 180-degree direction.

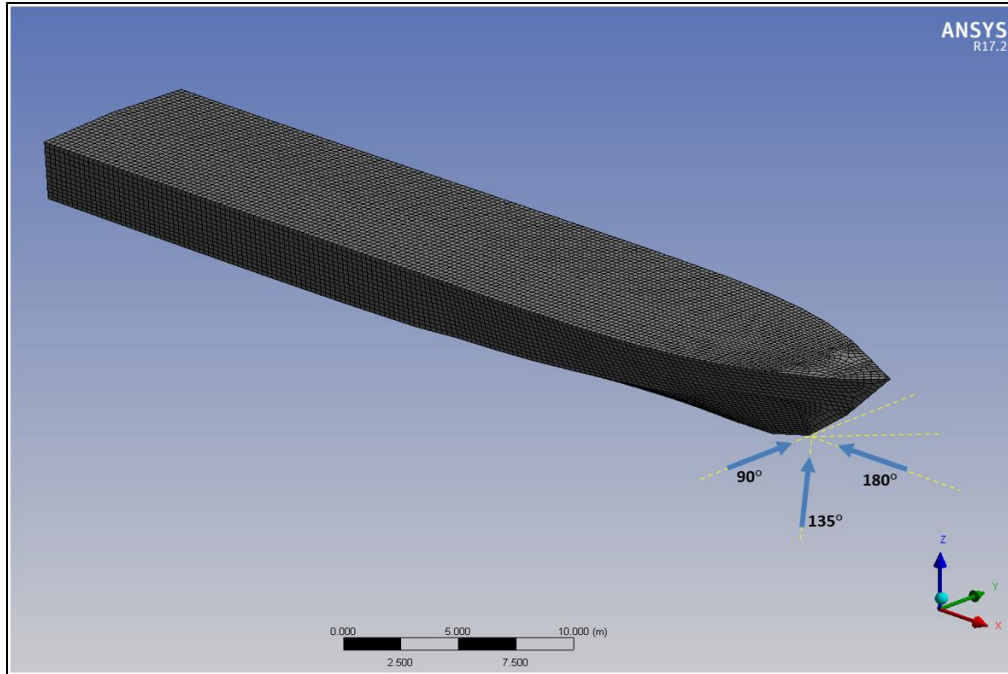


Figure 4-3: Hydrodynamic Analysis – Irregular Waves

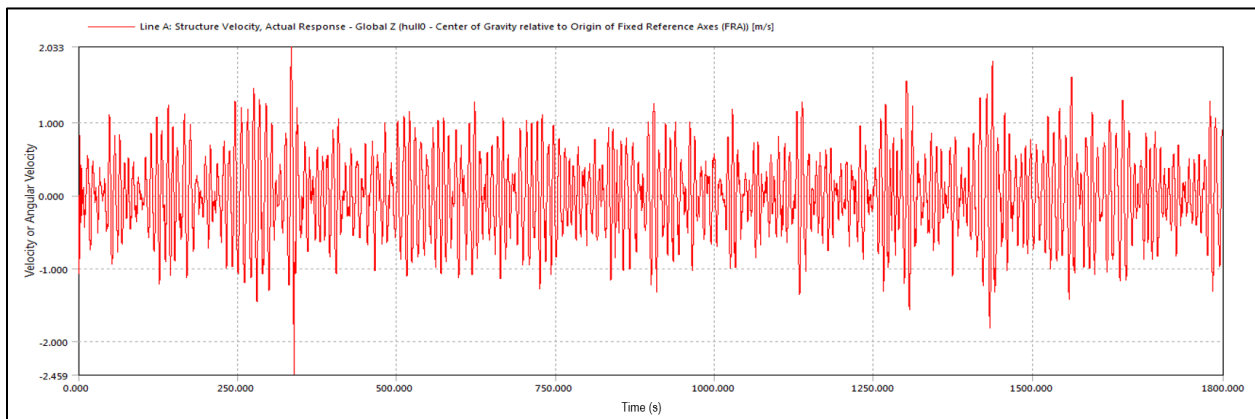


Figure 4-4: Structure Velocity vs. Time from the Hydrodynamic Analysis

In order to compute the slamming pressure acting on the bow portion of the vessel under transit conditions, a Computational Fluid Dynamics (CFD) analysis was performed using ANSYS FLUENT module to obtain the average pressure acting on the structure bottom under unit velocity of fluid, as shown in Figure 4-5. This figure represents a CFD domain in a stationary condition i.e. condition prior to the start of simulation. The CFD simulation was setup in such a way that the vessel is modeled to be stationary and it is subjected to 1 atmospheric air pressure and water velocity of 1m/s. The keel of the vessel is modeled at 1m above the water surface before the start of simulation.

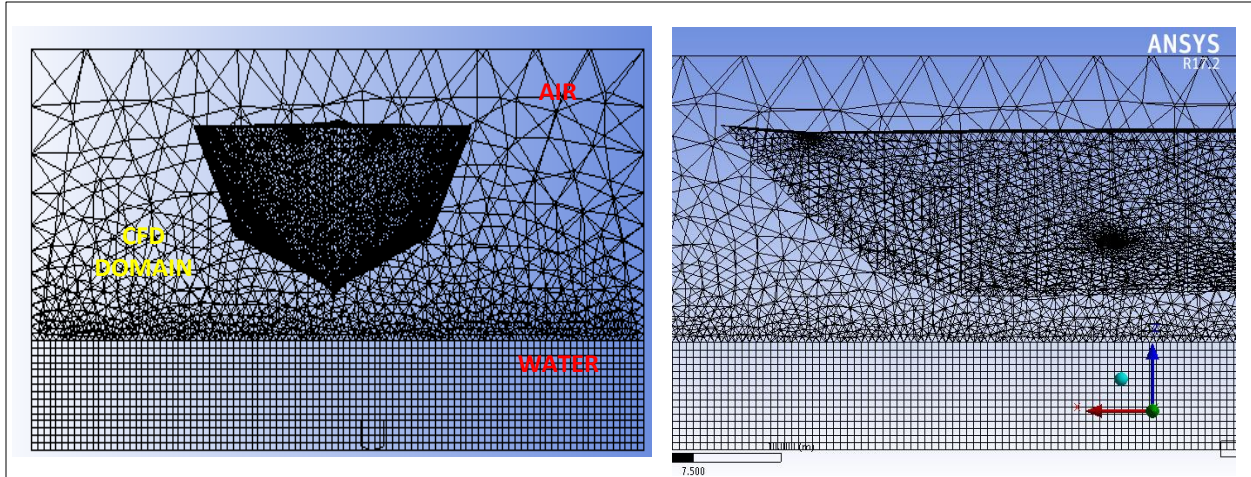


Figure 4-5: CFD Analysis to obtain Hydrodynamic Pressure under Unit Velocity

As the simulation begins, the vessel comes in contact with the fluids (air and water). The pressure time history over the length of simulation was recorded, and the time when the fluid comes in contact with the vessel represents a peak as indicated in Figure 4-7 and Figure 4-8 below, and further a unit slamming pressure was obtained from this step. Figure 4-6 below is a typical representation of the course of simulation, showing fluid contact with the vessel.

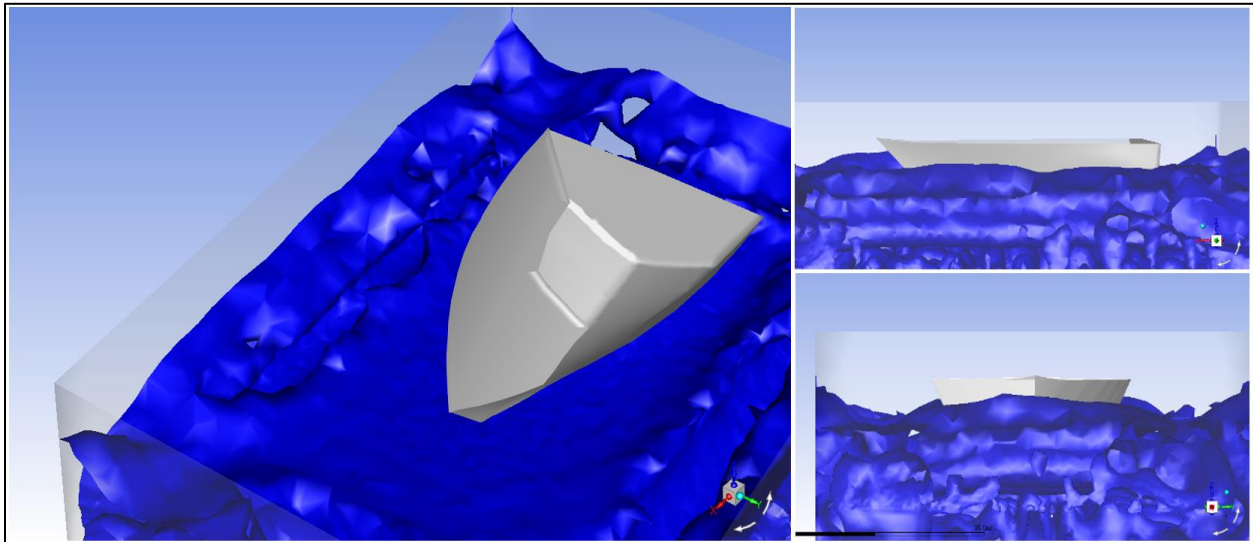


Figure 4-6: CFD Analysis – Representing Fluid Contact with the Vessel.

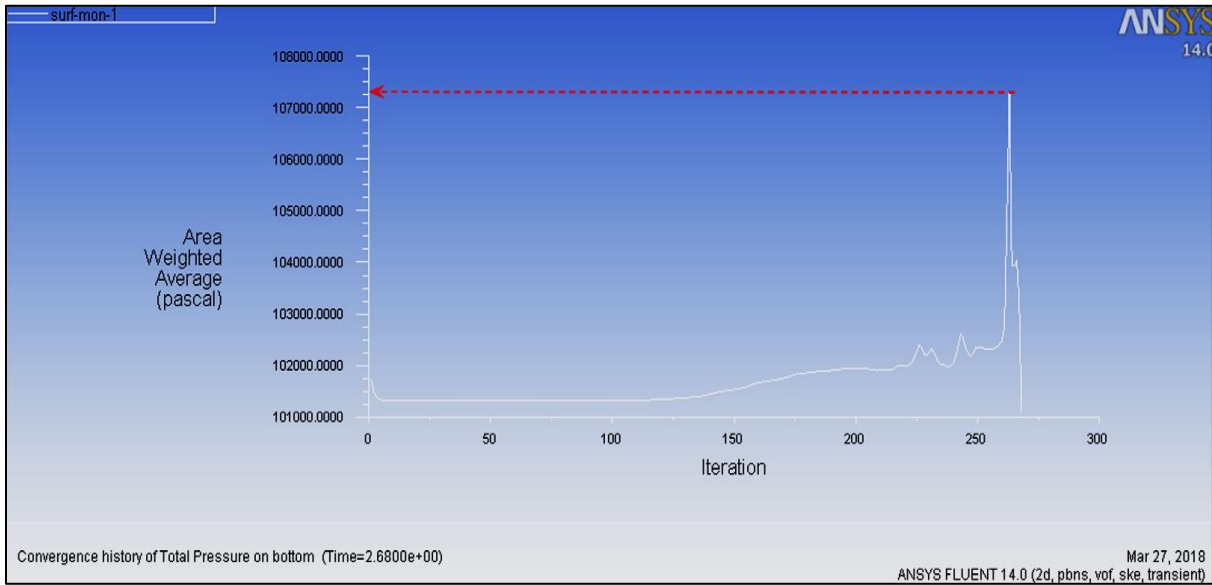


Figure 4-7: Plot for Average Slamming Pressure per unit Area over Time

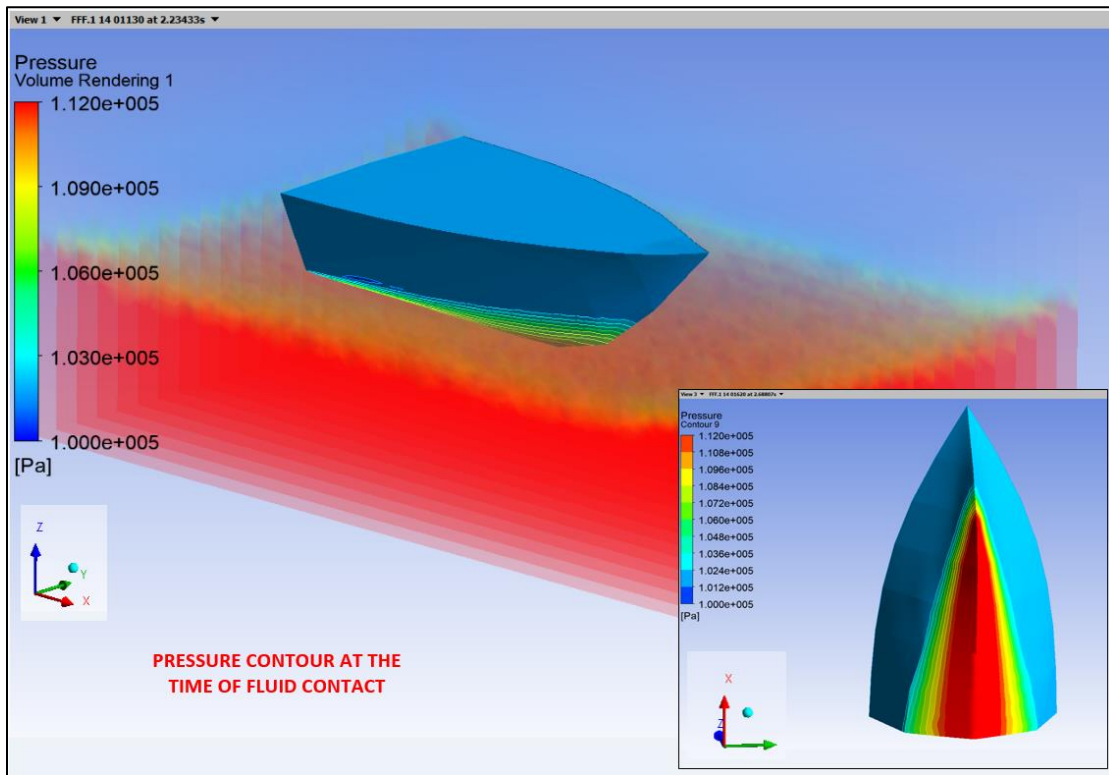


Figure 4-8: CFD Analysis – Pressure Contour at the time of Fluid Contact

Based on the obtained vessel response under transit conditions from irregular wave analysis and the average pressure per unit area from the CFD analysis, the design slamming pressure acting on the bow part of the hull was computed as below:

$$P_s = P_r * V_s^2$$

Where,

- P_s is the design slamming pressure,
- P_r is the resultant pressure (computed as, $P_r = \text{unit CFD pressure} - \text{air pressure of 1 atm}$),
- V_s is the structures velocity that varies with the wave direction and loading condition under consideration.

Figure 4-9 below represents the estimated slamming pressure under different loading conditions.

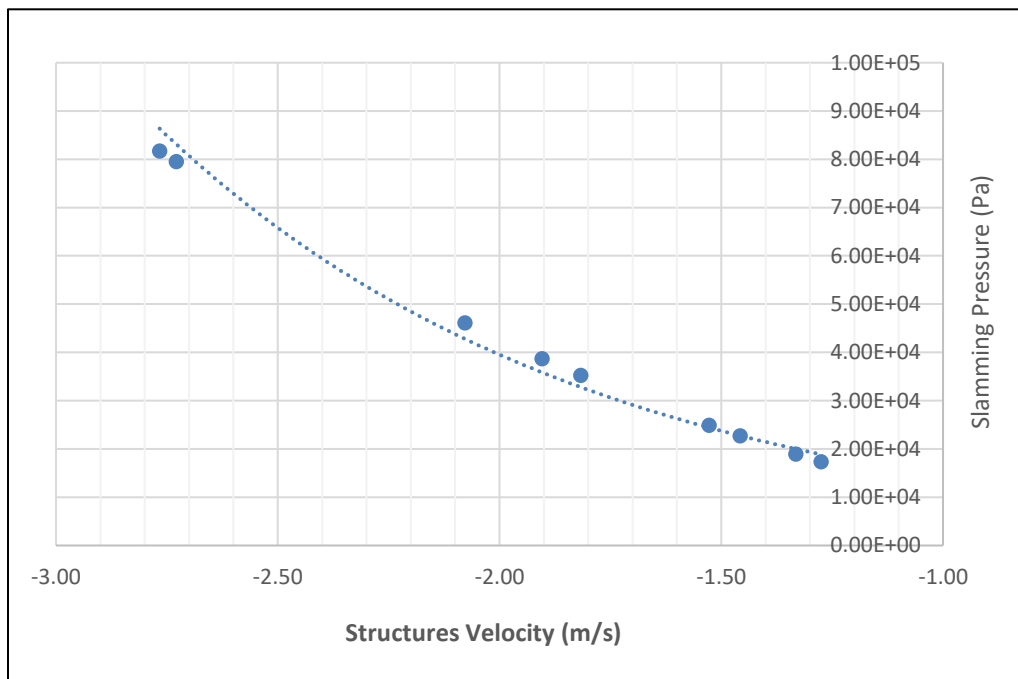


Figure 4-9: Slamming Pressure Estimate for Different Loading Conditions

In general, the computed slamming pressure on the bow part (acting on the hull bottom and the side shell) for the most critical loading conditions varied in the range of 11-12 psi and this value was applied to the entire bow region to identify the critical location for further crack propagation study.

4.4 Global FE Analysis

A global analysis was performed for the identified loading conditions detailed in section 4.3. Figure 4-10 and Figure 4-12 below represent the global model of the midship section (between frame 17 to frame 22) and Bow section (between frame 01 to 06) respectively, detailing the different structural elements such as the side shell and deck plating, stiffeners, transverse web framing, transverse and longitudinal bulkheads. Figure 4-11 represents the stress contour and the deformation of the midship section under the applied sagging and hogging bending moments performed using the FEMAP/NASTRAN Solver.

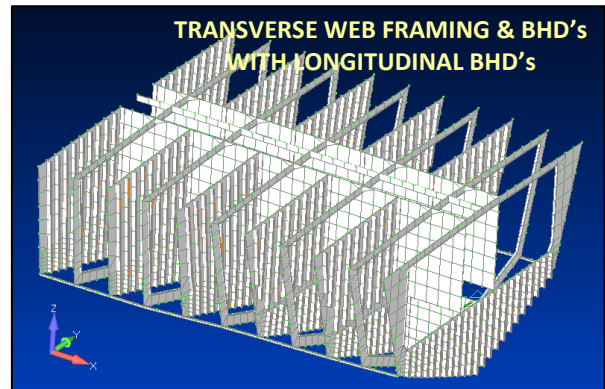
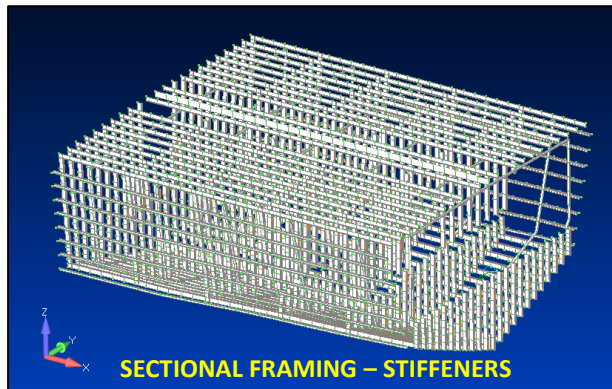
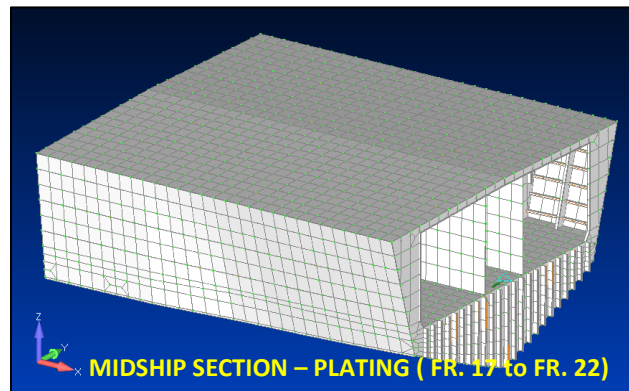


Figure 4-10: Global Model for the Midship Section

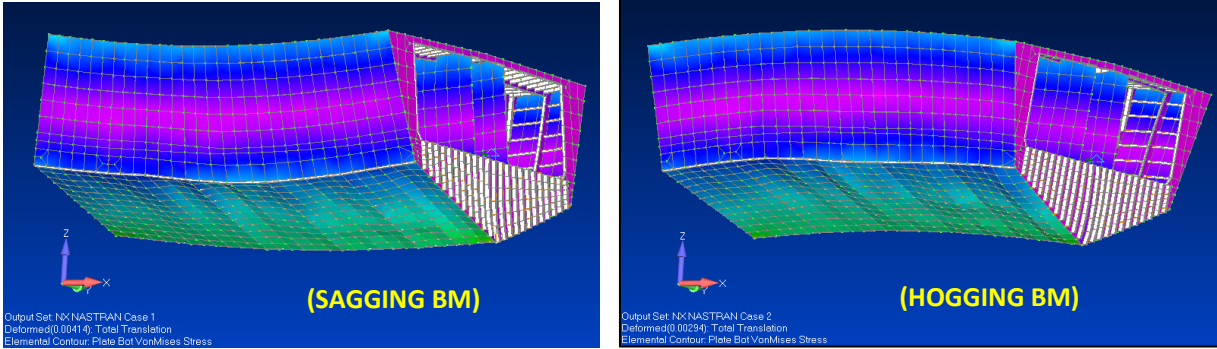


Figure 4-11: Vessel Stress Contours & Deformation due to Bending Moments

Figure 4-13 below represents the stress contour of the bottom shell plating of the bow section when subjected to slamming pressure at different frame and side shell locations (FR.01 to FR.06).

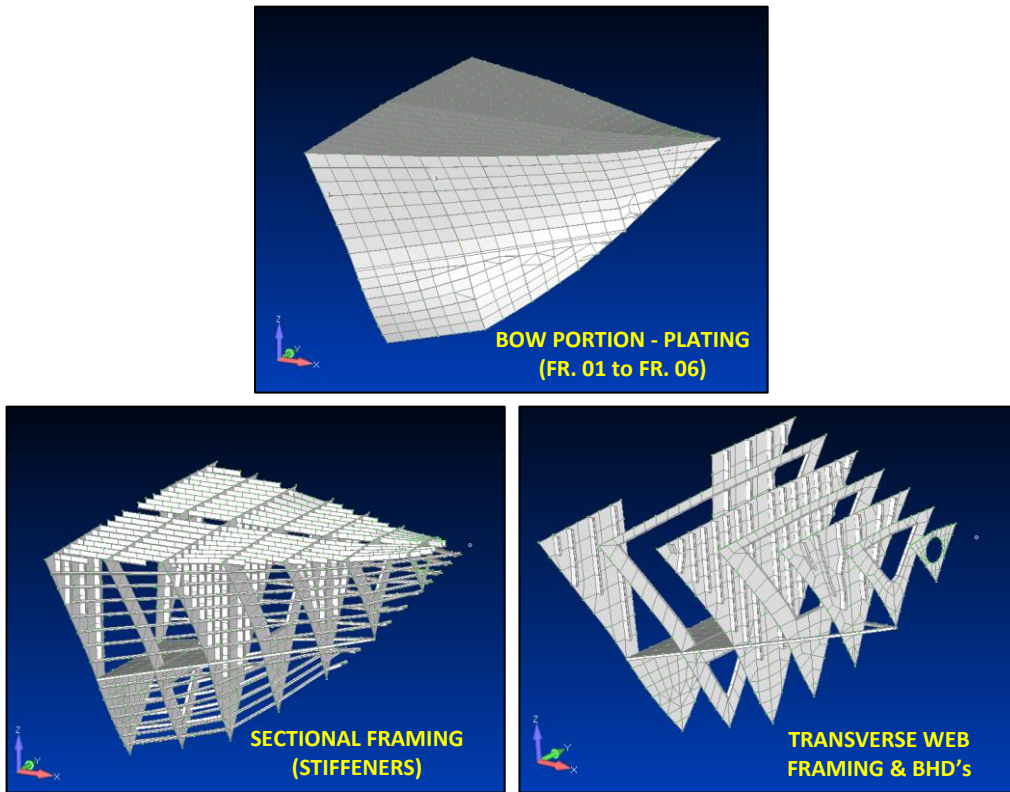


Figure 4-12: Global Model for the Bow Part

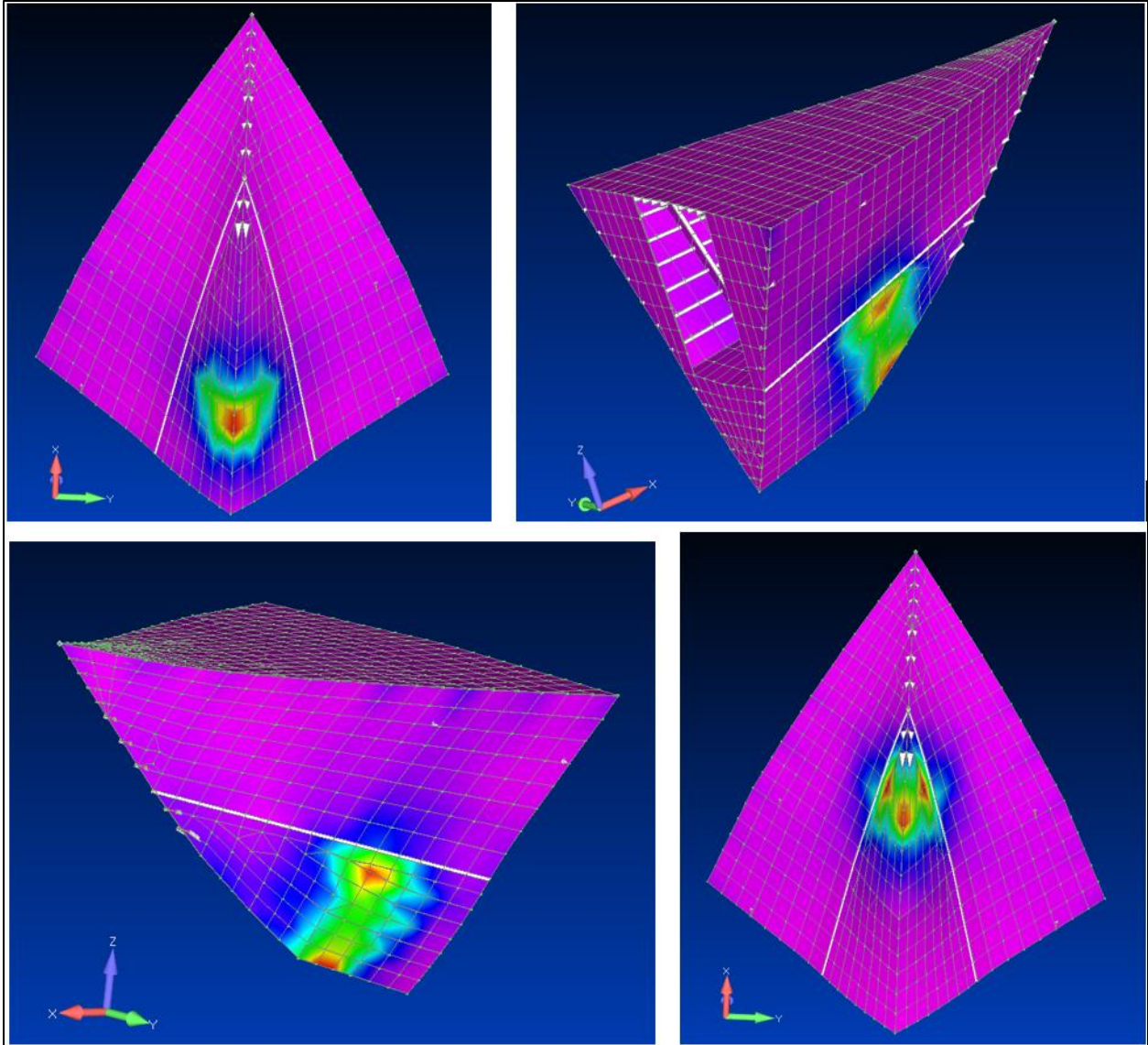
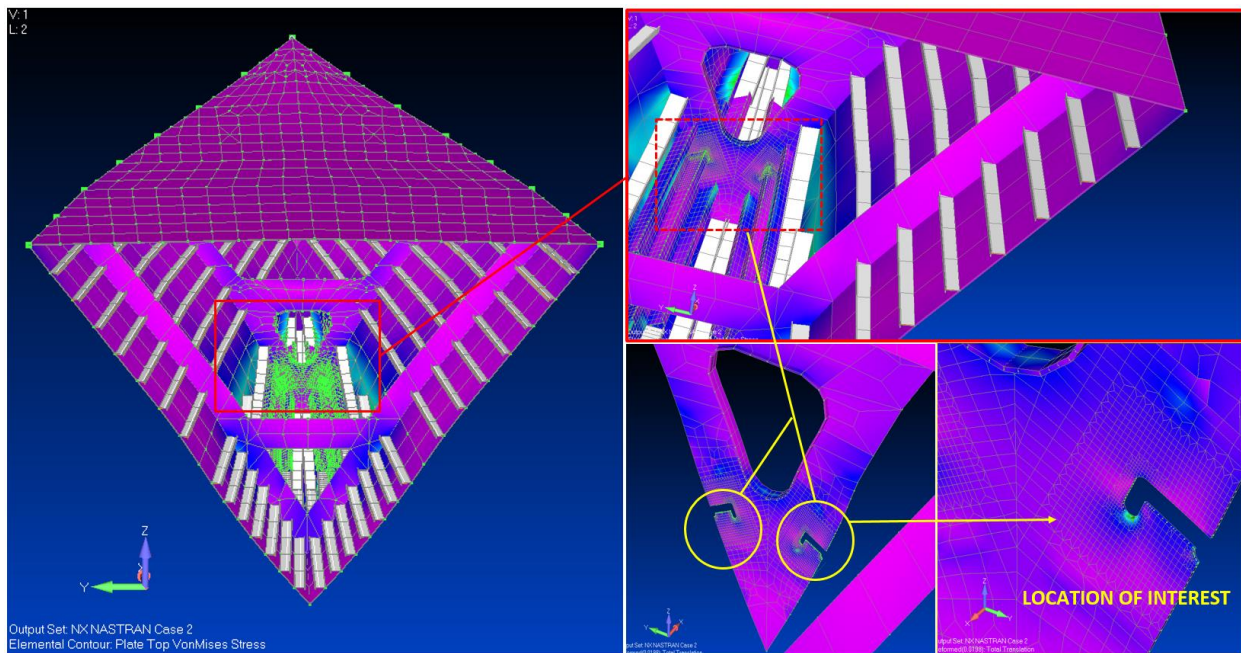


Figure 4-13: Stress Contour at the Bow Region due to Slamming Pressure

4.5 Critical Locations

Based on the results of the global analysis, the structural critical locations prone to crack initiation were identified and further detailed to obtain a localized stress field and nodal displacement that can be subsequently applied to a crack propagation local model. Also, critical loading conditions were shortlisted that are suitable for the crack propagation analysis. Figure 4-14 below represents the selected critical location on the fore part of the vessel that encompasses the Side Shell, Stiffener & Web frame regions. Figure 4-15 represents the critical location at the midship region encompassing the transverse web frame, bottom hull plating and the bottom stiffeners. Figure 4-16 demonstrates that, when a crack is locally introduced in a web plate of the transverse frame, the sagging bending moment in the midship section region will result in the crack tip closure while the hogging bending moment will result in the crack opening mode.



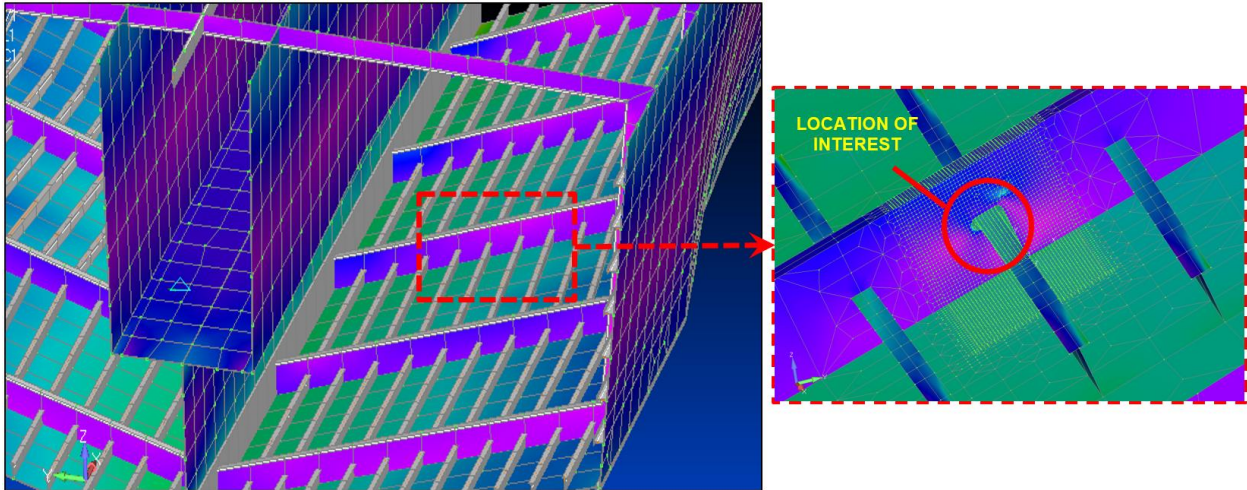


Figure 4-15: Local Model in the Critical Region of Bottom Web Frame (Midship Section)

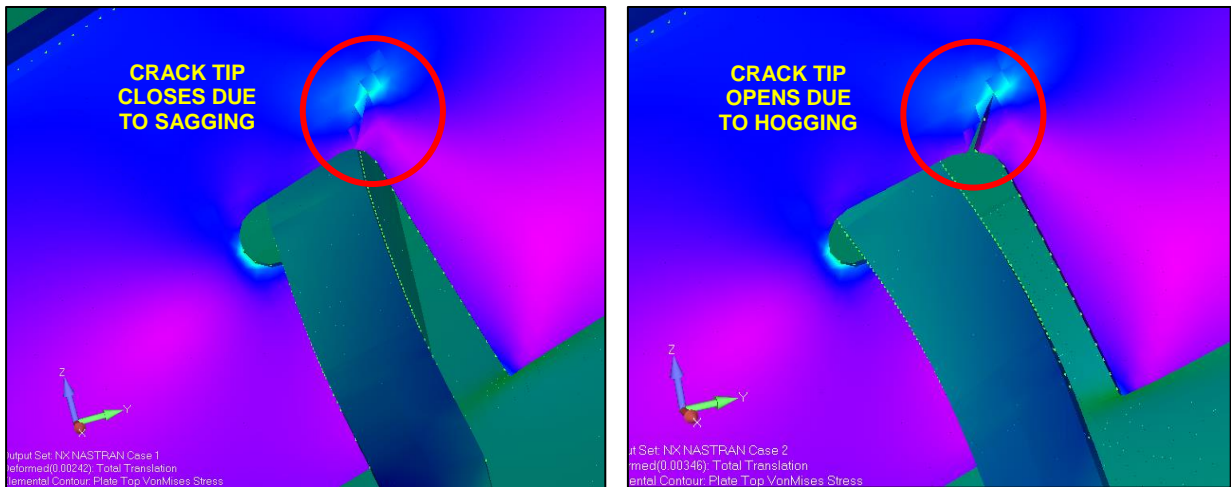


Figure 4-16: Crack Tip Behavior during the Sagging and Hogging Bending Moments

4.6 Crack Propagation Study

This section addresses the development of local FEA models for the crack propagation study in the midship and fore part region.

ABAQUS Software (Version-6.14) is utilized for conducting the crack propagation analysis. Specific details of the fracture mechanics methods used, throughout this report for the computation studies, are documented in the software's Analysis User's Guide [ref. 19].

4.6.1 Critical Midship Section

Based on the results of the global analysis, the critical location suitable for the crack opening mode was selected and a high-resolution local 3D finite element model was developed. Figure 4-17 below represents the web section of the bottom framing selected for crack propagation study with transformation from the coarse to a fine mesh (finest element size being $230\mu\text{m} \times 230\mu\text{m} \times 200\mu\text{m}$ thick). Figure 4-18 represents the plate elements transformed to the solid elements, along with the application of nodal displacement to this local FEA model as boundary conditions obtained from the global analysis under the Hogging Bending Moment Scenario that triggers the crack opening mode.

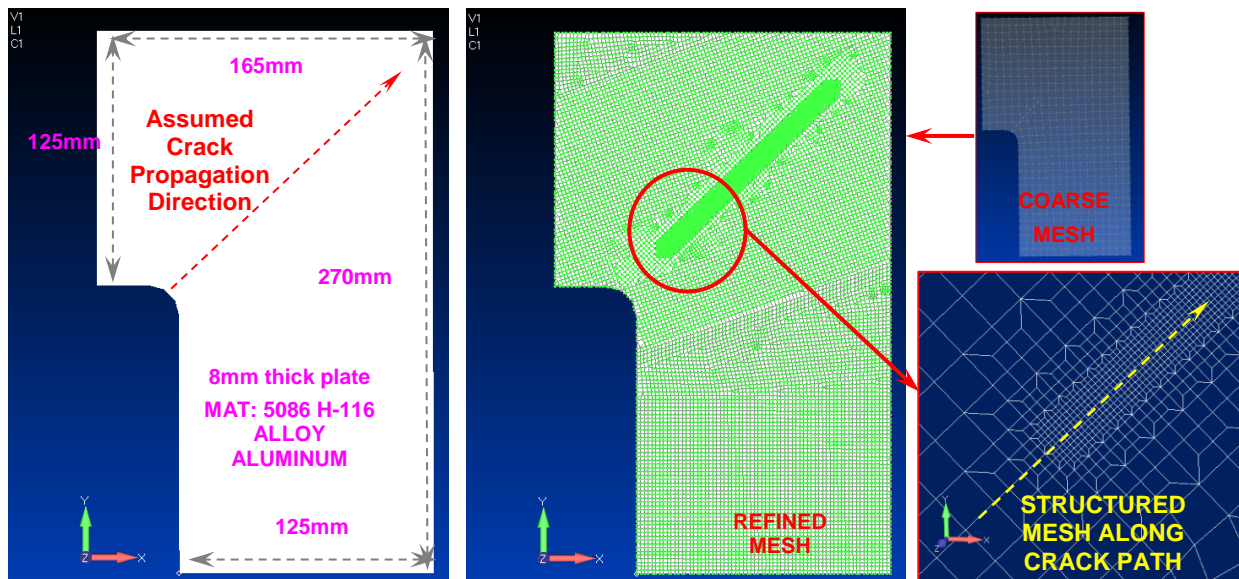


Figure 4-17: Extracted Web Section - Refined for Crack Propagation Study – Midship Section

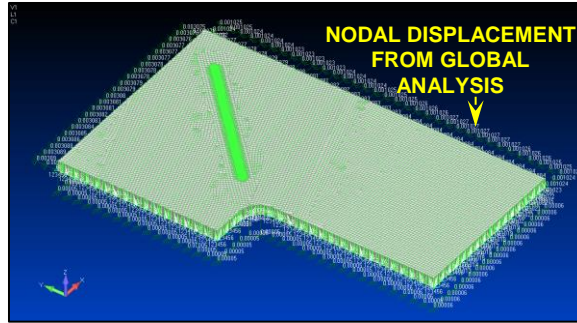


Figure 4-18: Conversion from Plate to Solid Elements and Application of Nodal displacements

This high-resolution local FE model was subsequently exported to the ABAQUS software for further evaluation of the Stress Intensity Factors (SIF) using the Contour Integral Method. Figure 4-19 demonstrates the introduction of a crack front at 25mm from the free end and a crack propagation direction. This step was repeated for each 25mm increment to the crack length starting from 25mm to 125mm. At each step the SIF was obtained. The SIFs obtained using the contour integral method represents the maximum energy released associated with the crack propagation. The Abaqus model was set up to deliver SIF for 5 successive contours initiating from the crack tip location.

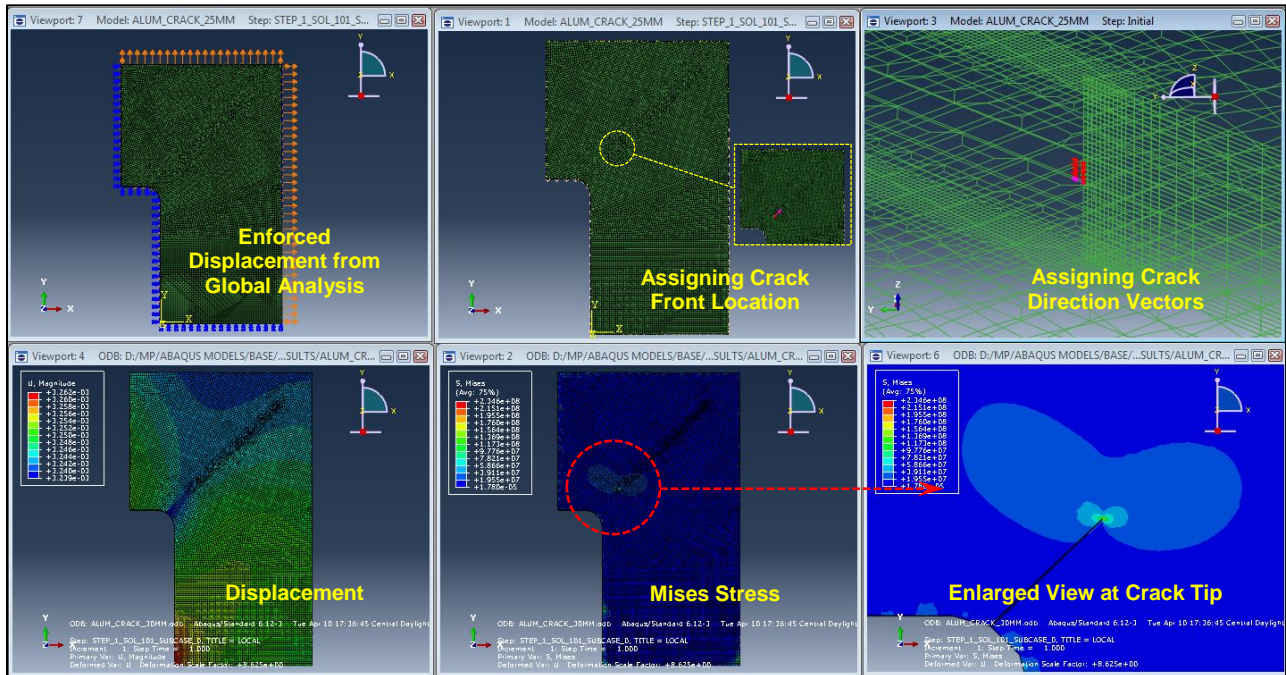


Figure 4-19: Obtain SIF using Contour Integral Method (Model with 25mm Crack Length Shown)

Figure 4-20 below represents the von Mises stress contour for progressively increasing crack lengths, whereas Figure 4-21 is the same plot but an enlarged view at the crack tip region.

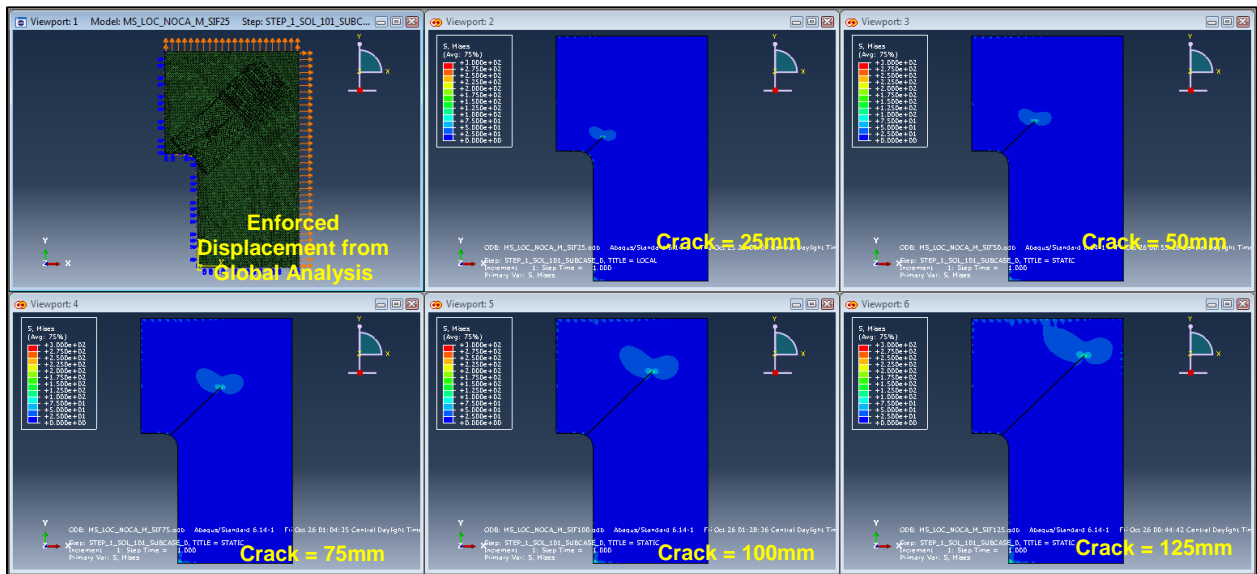


Figure 4-20: Von Mises Stress Contour for Progressively Increasing Crack Lengths – Midship Section

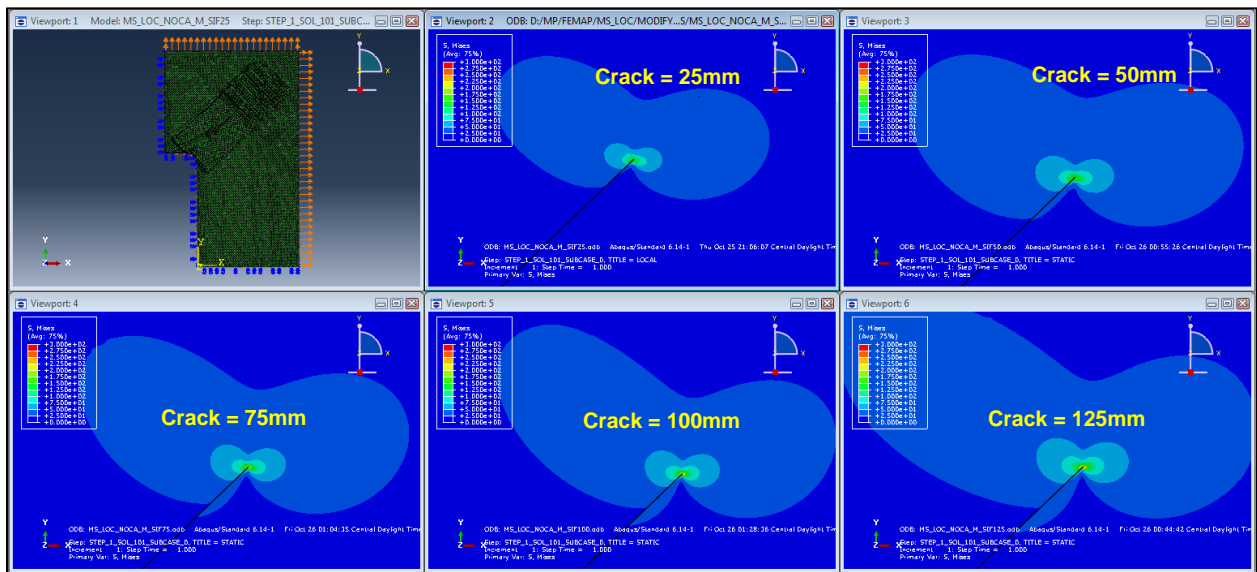


Figure 4-21: Von Mises Stress Contour for Different Crack Lengths (focused at crack tip region) - Midship Section

Table 4-4 below represents the SIF's obtained from the CIM (Contour Integral Method) for different crack lengths. K1, K2 & K3 in the table represents the stress intensity factors for three (3) modes of crack extension, respectively Mode-I (Crack Opening), Mode-II (In-plane Shearing or Sliding) and Mode-III (Out-of-Plane Tearing).

It is observed that for all the cases K1 mode (Crack Opening) is typically dominant. Additionally, the SIF values converge after the third contour integral thus the SIF's from 3rd contour was used for further evaluation purposes.

Table 4-4 : SIF Output for Different Crack Lengths with Contour Integral Method – Midship

CRACK LENGTH = 25mm				CRACK LENGTH = 50mm			
Contour	K1	K2	K3	Contour	K1	K2	K3
1	4.161	1.890	0.114	1	4.495	2.460	0.148
2	4.449	1.957	0.124	2	4.806	2.547	0.162
3	4.464	1.962	0.124	3	4.820	2.553	0.162
4	4.466	1.962	0.125	4	4.823	2.553	0.164
5	4.466	1.962	0.126	5	4.823	2.553	0.164
CRACK LENGTH = 75mm				CRACK LENGTH = 100mm			
Contour	K1	K2	K3	Contour	K1	K2	K3
1	5.249	3.002	0.181	1	5.692	3.381	0.200
2	5.612	3.108	0.198	2	6.087	3.502	0.219
3	5.629	3.117	0.198	3	6.104	3.508	0.219
4	5.632	3.117	0.200	4	6.107	3.508	0.221
5	5.632	3.117	0.200	5	6.110	3.508	0.221
CRACK LENGTH = 125mm				SUMMARY - SIF range in Stress in Mpa.m ^{1/2}			
Contour	K1	K2	K3	Crack (mm)	ΔK1	ΔK2	ΔK3
1	6.078	3.750	0.217	25	8.927	3.923	0.249
2	6.498	3.879	0.238	50	9.641	5.106	0.325
3	6.515	3.888	0.238	75	11.258	6.233	0.396
4	6.518	3.888	0.240	100	12.208	7.016	0.439
5	6.521	3.888	0.241	125	13.031	7.776	0.477

In order to account for the bi-axial or the mixed mode loading, an Effective Stress Intensity Factor (K_{eff}) is calculated as follows:

$$K_{eff} = \{K_1 + K_2 + K_3 / (1-\nu)\}^{1/2}$$

where, ' ν ' is the Poisson's Ratio.

Figure 4-22 below represents the polynomial curve fitted to represent the SIF range corresponding to different crack lengths.

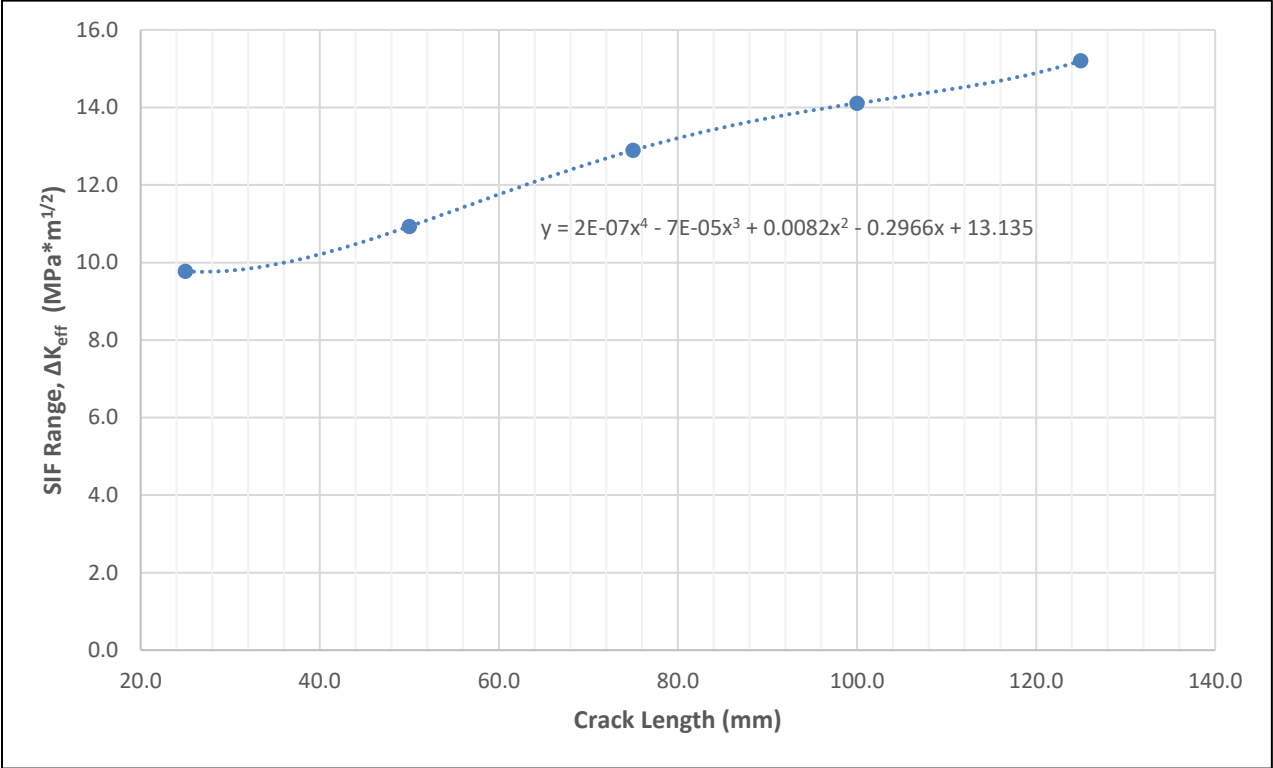


Figure 4-22: SIF Range, ΔK_{eff} vs. Crack Length (mm) – Midship Section

4.6.2 Critical Bow Section

Similar to the midship section, a local high-resolution model was developed for the critical bow section. Figure 4-23 below represents the web section of the bottom framing selected for crack propagation study with transformation from the coarse to a finer mesh development with further introduction of the enforced displacement from the global analysis to match the stress field.

Further a SIF evaluation was performed using CIM (Contour Integral Method) for different crack lengths, implementing the same methodology adopted for the midship section. For all the cases, K2 (in-plane shearing) mode was found to be typically dominant.

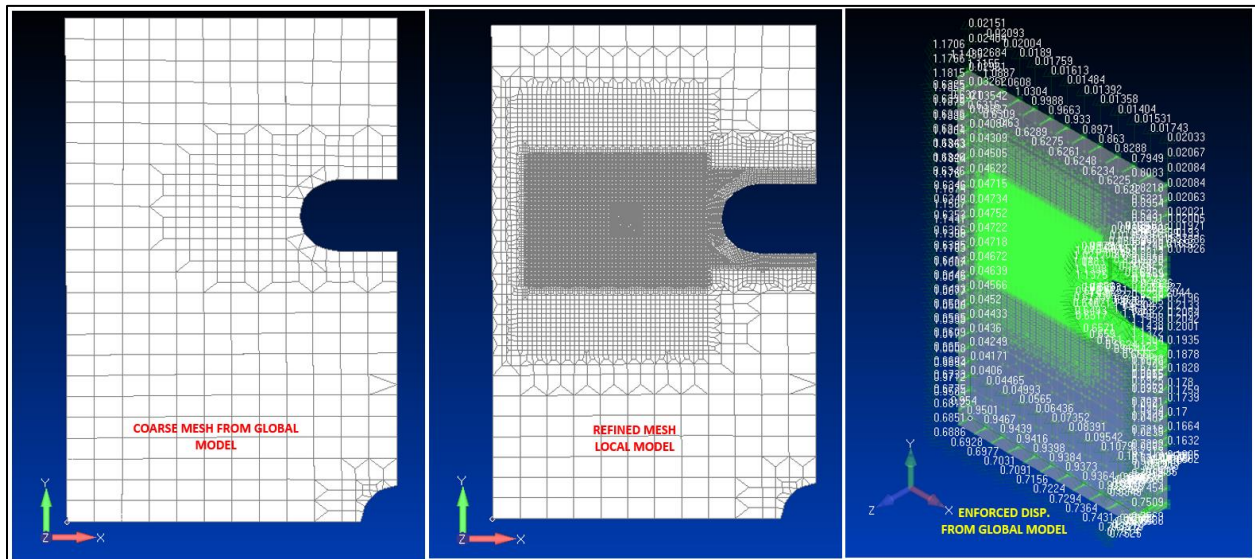


Figure 4-23: Extracted Web Section - Refined for Crack Propagation Study– Bow Section

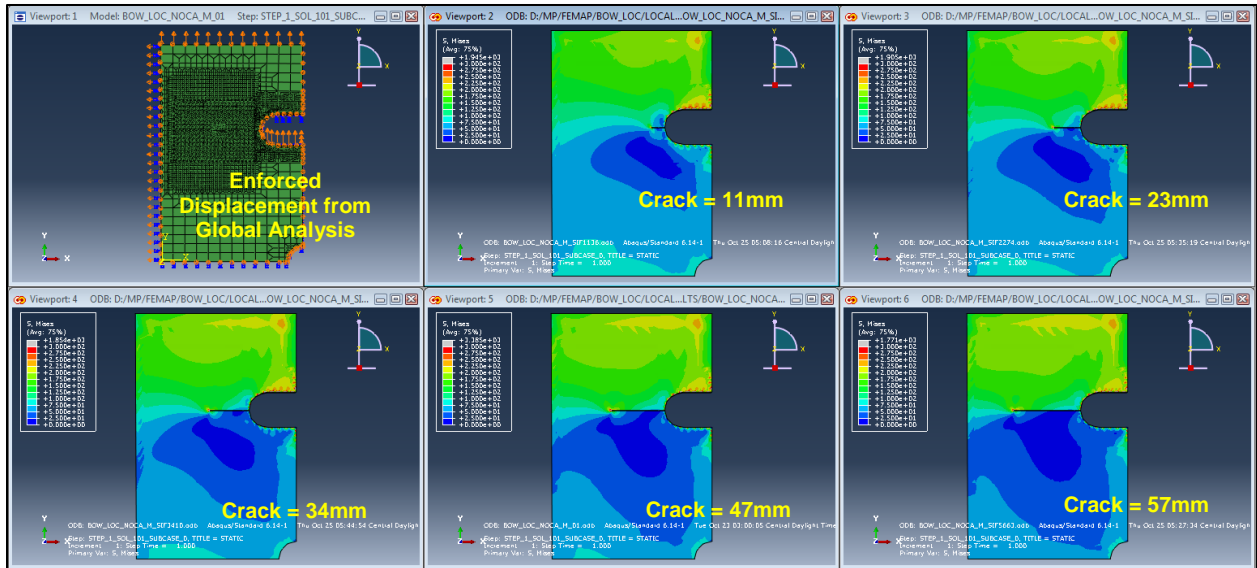


Figure 4-24: Von Mises Stress Contour for Progressively Increasing Crack Lengths – Bow Section

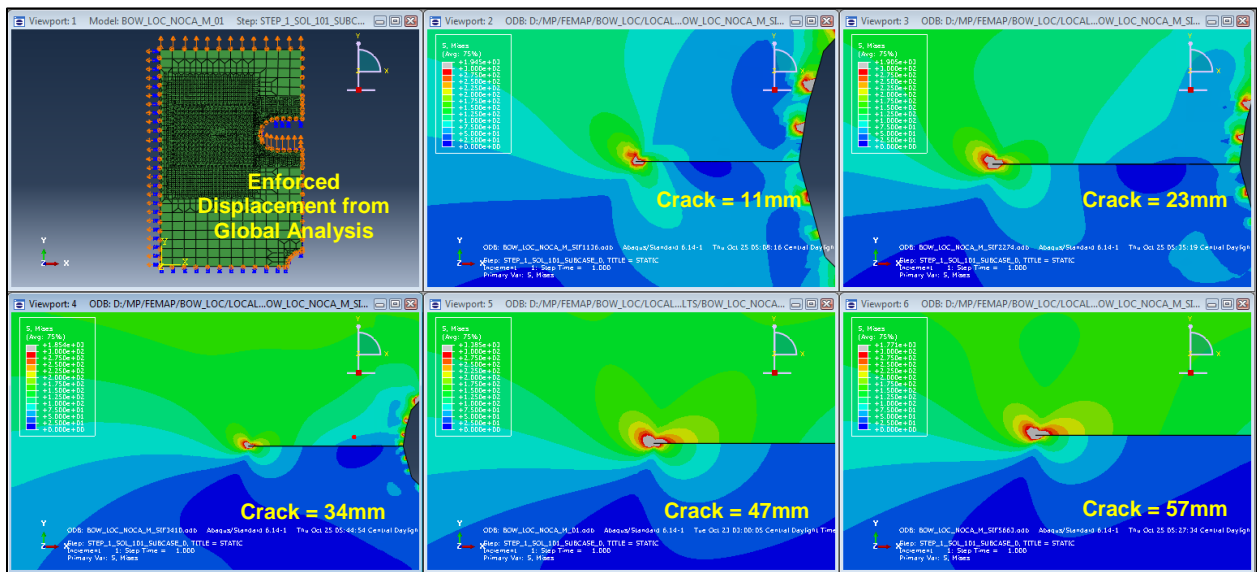


Figure 4-25: Von Mises Stress Contour for Different Crack Lengths (focused at crack tip region) – Bow Section

Table 4-5 : SIF Output for Different Crack Lengths with Contour Integral Method – Bow

CRACK LENGTH = 11mm				CRACK LENGTH = 23mm			
Contour	K1	K2	K3	Contour	K1	K2	K3
1	5.865	6.599	2.758	1	3.937	10.288	3.868
2	5.865	6.602	2.757	2	3.937	10.291	3.865
3	5.862	6.602	2.757	3	3.937	10.294	3.865
4	5.862	6.602	2.757	4	3.934	10.294	3.865
5	5.862	6.602	2.757	5	3.934	10.294	3.865
CRACK LENGTH = 34mm				CRACK LENGTH = 47mm			
Contour	K1	K2	K3	Contour	K1	K2	K3
1	2.797	11.897	4.325	1	2.220	11.249	4.518
2	2.796	11.908	4.328	2	2.283	12.418	4.927
3	2.796	11.900	4.325	3	2.291	12.409	4.826
4	2.796	11.906	4.325	4	2.293	12.409	4.740
5	2.794	11.900	4.325	5	2.293	12.406	4.671
CRACK LENGTH = 57mm				SUMMARY - SIF range in Stress in Mpa.m ^{1/2}			
Contour	K1	K2	K3	Crack (mm)	ΔK1	ΔK2	ΔK3
1	1.494	11.756	4.216	11	11.724	13.203	5.514
2	1.494	11.759	4.213	23	7.874	20.588	7.730
3	1.494	11.762	4.213	34	5.592	23.800	8.651
4	1.493	11.762	4.213	47	4.583	24.818	9.652
5	1.493	11.762	4.213	57	2.987	23.523	8.426

Figure 4-26 below represents the polynomial curve fitted to represent the SIF range corresponding to different crack lengths.

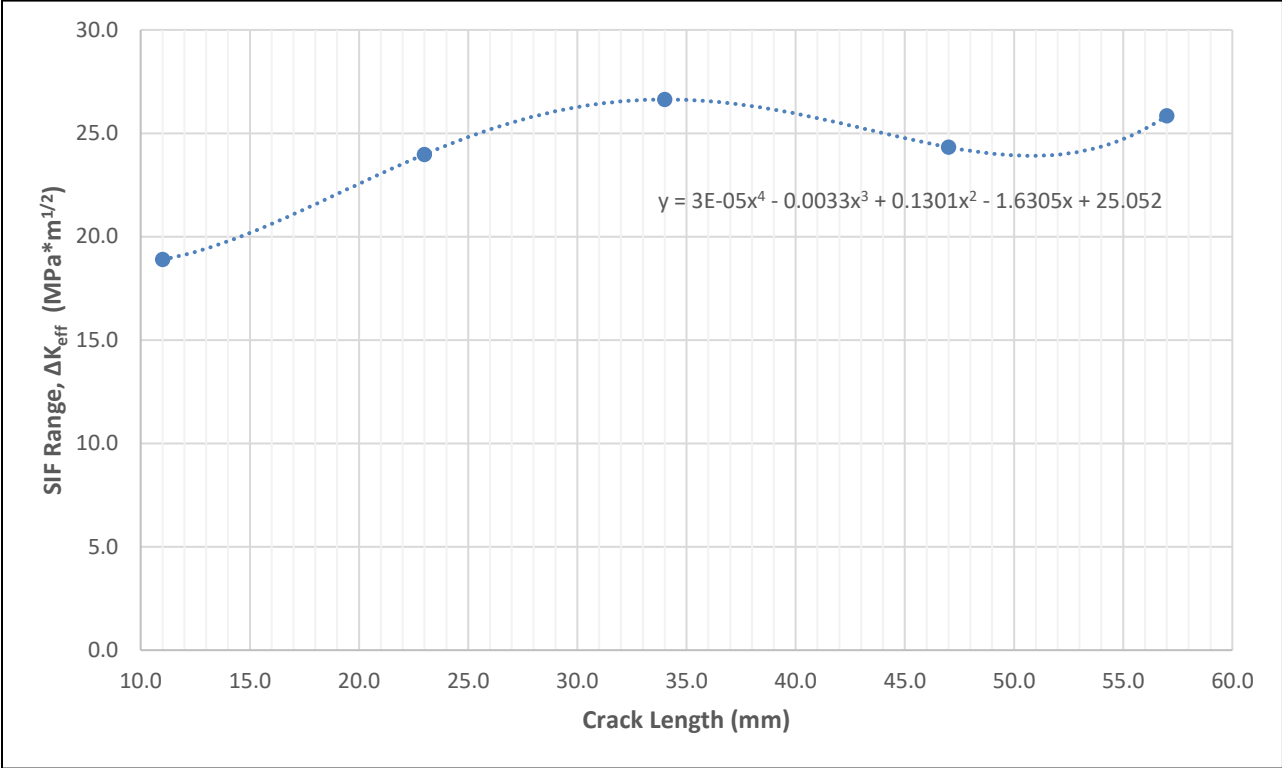


Figure 4-26: SIF Range, ΔK_{eff} vs. Crack Length (mm) – Bow Section

5 Development of Crack Arrestor Models

In order to have a more controlled loading and subsequently standardize the results, a calibration model analogous to a typical compact test specimen was considered as an initial step for the development and evaluation of different crack arrestors. For the test data of fracture toughness and fatigue crack growth rate, SSC 448/ SR-1447 issued documents were used for reference and validation purposes for a specimen without a crack arrestor. The Compact Tension (CT) specimen with a known crack length and loading conditions, was then modulated by introducing different arrestors at the crack tip as shown in Figure 5-1. Please note that all specimens below have a constant crack length of 1.6 inch (40 mm) and the thickness of the specimen is 8mm.

The following (5) types of crack arrestors were studied, and they are discussed in detail in the subsequent sections:

- TYPE-1 - CAH (Crack Arrest Hole)
- TYPE-2 - CAH (Crack Arrest Hole) with Interference Bolt
- TYPE-3 - CAH (Crack Arrest Hole) with Bolted Patch Plate
- TYPE-4 - CAH (Crack Arrest Hole) with Welded Patch Plate
- TYPE-5 - CAH (Crack Arrest Hole) with Interference Bolt & Welded Patch Plate

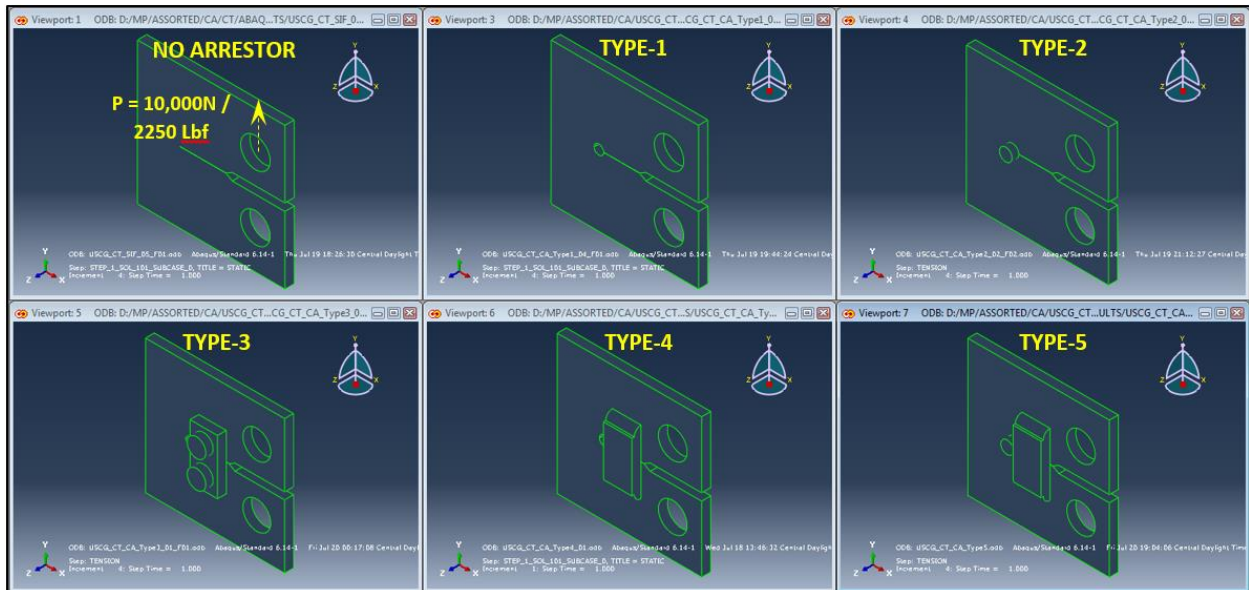


Figure 5-1: Different Crack Arrestors Considered for Study

5.1 Base Study Specimen without a Crack Arrestor

All the crack arrestors mentioned in the above section are studied with the following base specimen as shown in Figure 5-2. The bottom pin location was fixed and the load of 10kN was applied at the top pin. The stress intensity factor SIF at the crack tip (with 40 mm length from the notch) was evaluated with the same methodology as explained in Section 4.6.1.

The material properties of the specimen under considerations are as follows

Table 5-1 : Material Properties

Aluminum Alloy	5086-H116
Plate Thickness	8 mm
Elastic Modulus	71000 Mpa
Poisson's Ratio	0.33
Threshold Intensity Range, ΔK_{th}	~3 Mpa \sqrt{m}
Critical Intensity Range, ΔK_{Ic}	~44 Mpa \sqrt{m}
Load (P)	10 KN

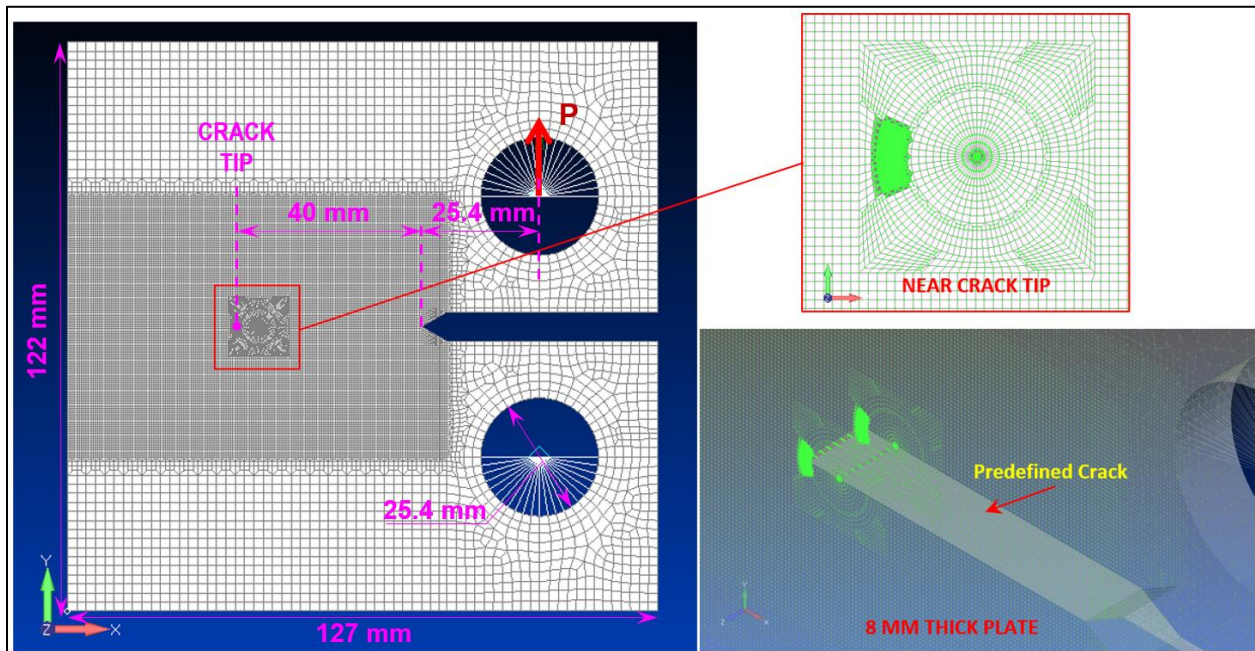


Figure 5-2: Base Specimen without a Crack Arrestor

5.2 CRACK ARRESTOR TYPE-1 - CAH (Crack Arrest Hole)

Figure 5-3 represents the type-1 arrestor i.e. with a Crack Arrest Hole (CAH) of 0.325" (8.255 mm). The diameter of the CAH is the same as that of the thickness of the plate. The loading condition was maintained the same as per the base specimen, refer Section 5.1, and the stress intensity factor SIF at the crack tip (same as 40 mm length from the notch) was evaluated.

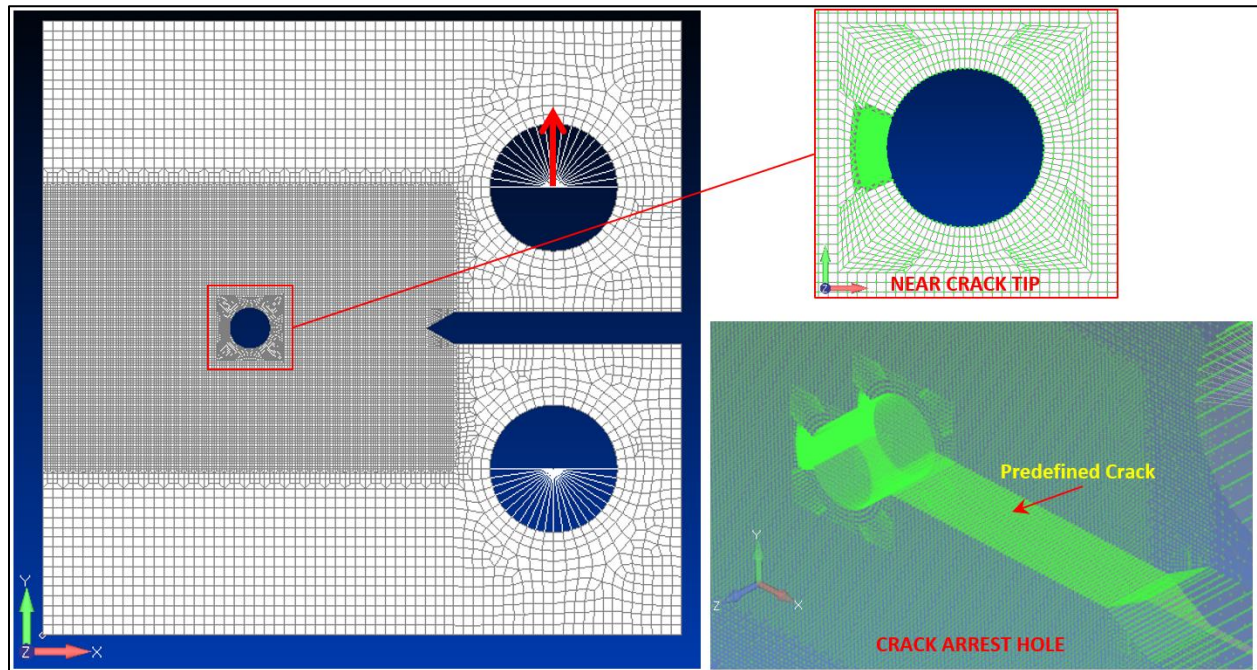


Figure 5-3: CRACK ARRESTOR TYPE-1 - CAH (Crack Arrest Hole)

Note: In the present study, an arbitrary slit of length 0.5 mm is introduced after the CAH in order to obtain the SIF at the same location (or to have a common location / monitoring point for evaluation) of different type of crack arrestors. In practice, when the repair technique is being employed in the field, NO slit or a tip shall be left behind the CAH.

5.3 CRACK ARRESTOR TYPE-2 - CAH with Interference Bolt

Figure 5-4 represents the type-2 arrestor i.e. Crack Arrest Hole (CAH) of 0.325" (8.255 mm) with introduction of a preloaded bolt, to create a compressive stress field at the crack tip region, using an Interference Bolt with a pin diameter same as the CAH. The Interference Bolt is secured by a washer and nut on the other end of the plate. The loading condition was maintained the same as per the base specimen, refer Section 5.1, and the stress intensity factor SIF at the crack tip (same as 40 mm length from the notch) was evaluated.

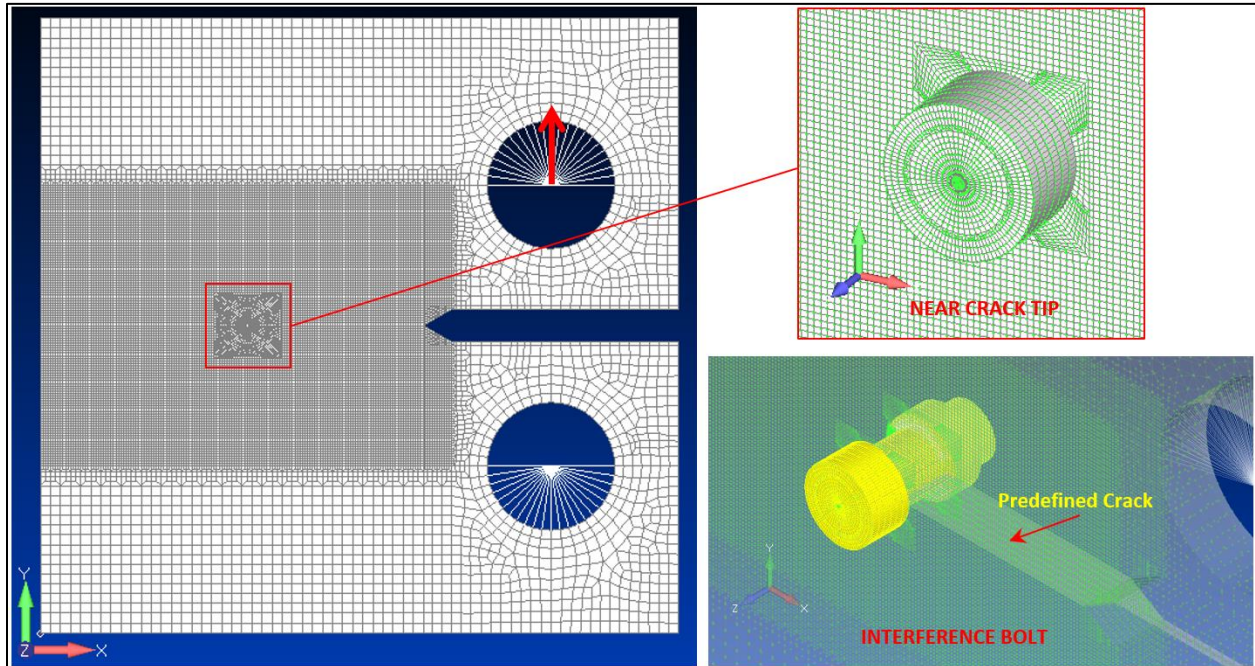


Figure 5-4: CRACK ARRESTOR TYPE-2 - CAH (Crack Arrest Hole) with Interference Bolt

Metric 8mm (M8) grade 8.8 bolt was considered for the study purpose with an applied preload of 10kN. The specification for the bolts, washer and nuts were assumed to meet ASTM A325 grade.

5.4 CRACK ARRESTOR TYPE-3 - CAH with Bolted Patch Plate

Figure 5-5 below represents the type-3 arrestor i.e. a Crack Arrest Hole (CAH) of 0.325" (8.255 mm) with introduction of a bolted patch plate. The patch plate thickness and material were maintained same as that of the specimen material i.e. 8mm thick Aluminum alloy 5085 H116. The size of the patch plate used was 25mm x 50mm and the same was bolted to the specimen using M10 bolts (Metric 10mm). A bolt preload of 10kN each was applied. The specification for the bolts, washer and the nuts were assumed to meet ASTM A325 grade.

The loading condition was maintained the same as per the base specimen, refer Section 5.1, and the stress intensity factor SIF at the crack tip (same as 40 mm length from the notch) was evaluated.

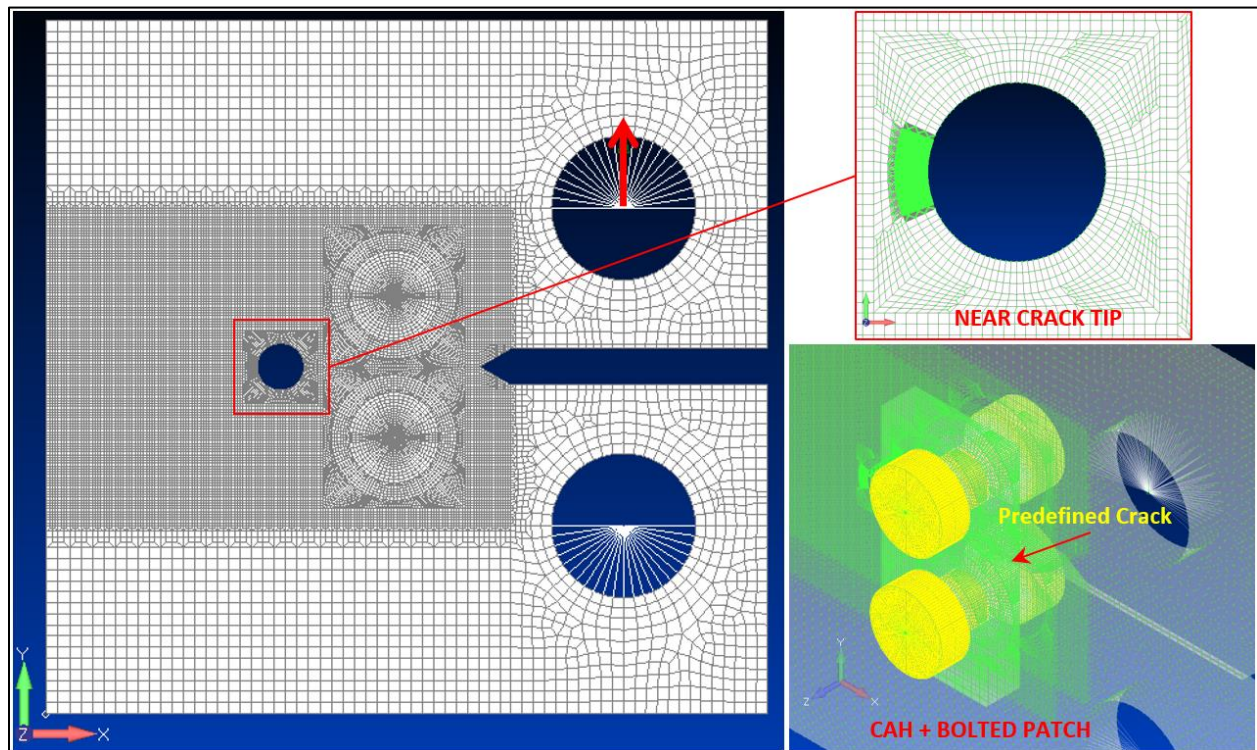


Figure 5-5: CRACK ARRESTOR TYPE-3 - CAH (Crack Arrest Hole) with Bolted Patch Plate

5.5 CRACK ARRESTOR TYPE-4 - CAH with Welded Patch Plate

Figure 5-6 below represents the type-4 arrestor i.e. a Crack Arrest Hole (CAH) of 0.325" (8.255 mm) with introduction of a welded patch plate. The patch plate thickness and material were maintained same as that of the specimen material i.e. 8mm thick Aluminum alloy 5085 H116. The size of the patch plate used was 25mm x 50mm.

The loading condition was maintained the same as per the base specimen, refer Section 5.1, and the stress intensity factor SIF at the crack tip (same as 40 mm length from the notch) was evaluated.

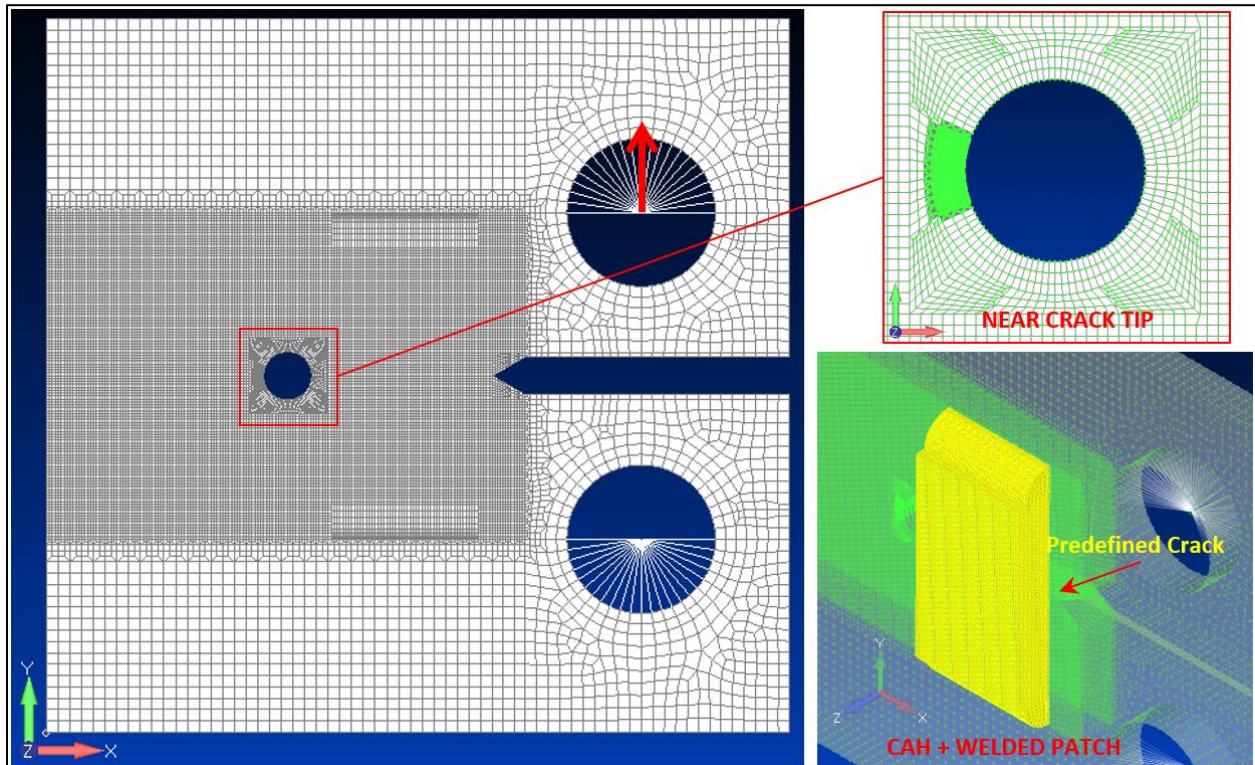


Figure 5-6: CRACK ARRESTOR TYPE-4 - CAH (Crack Arrest Hole) with Welded Patch Plate

5.6 CRACK ARRESTOR TYPE-5 - CAH with Interference Bolt & Welded Patch Plate

Figure 5-7 below represents a Type-5 arrestor that is a combination of Type-2 and Type-4. This arrestor, type-5, was included in study since arrestor Type-4 alone presented lower performance when compared to Type-2 & Type-3.

The arrestor has a Crack Arrest Hole (CAH) of 0.325" (8.255 mm) with an interference bolt of metric 8mm (M8) size, grade 8.8, with an applied bolt preload of 10kN. The specification for the bolts, washer and nuts were assumed to meet ASTM A325 grade. The patch plate thickness and material were maintained same as that of the specimen material i.e. 8mm thick Aluminum alloy 5085 H116. The size of the patch plate used was 25mm x 50mm.

The loading condition was maintained the same as per the base specimen, refer Section 5.1, and the stress intensity factor SIF at the crack tip (same as 40 mm length from the notch) was evaluated.

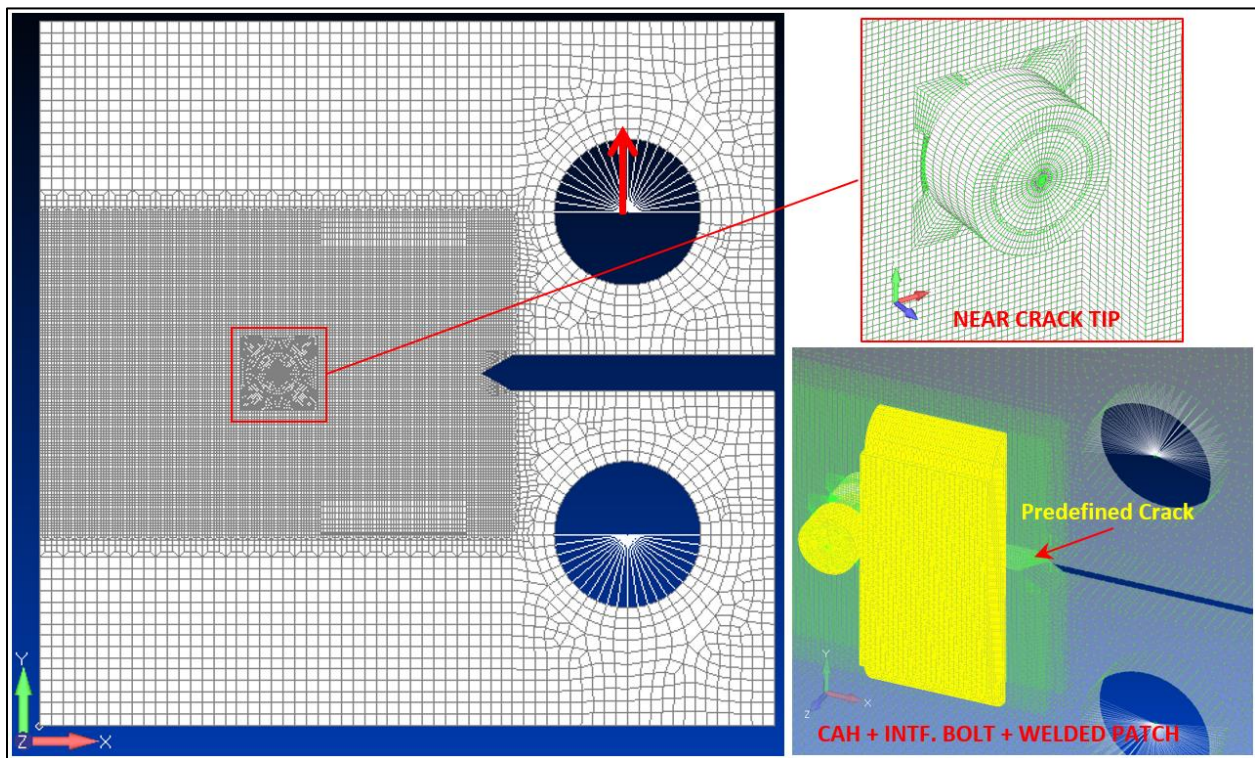


Figure 5-7: CRACK ARRESTOR TYPE-5 - CAH (Crack Arrest Hole) with Interference Bolt & Welded Patch Plate

Figure 5-8 below represents the von Mises stress contour for different studied crack arrestors, whereas Figure 5-9 below represents the stress contour at the crack tip region showing the variation in the magnitude of plastic zone at the crack tip region with the introduction of different crack arrestors.

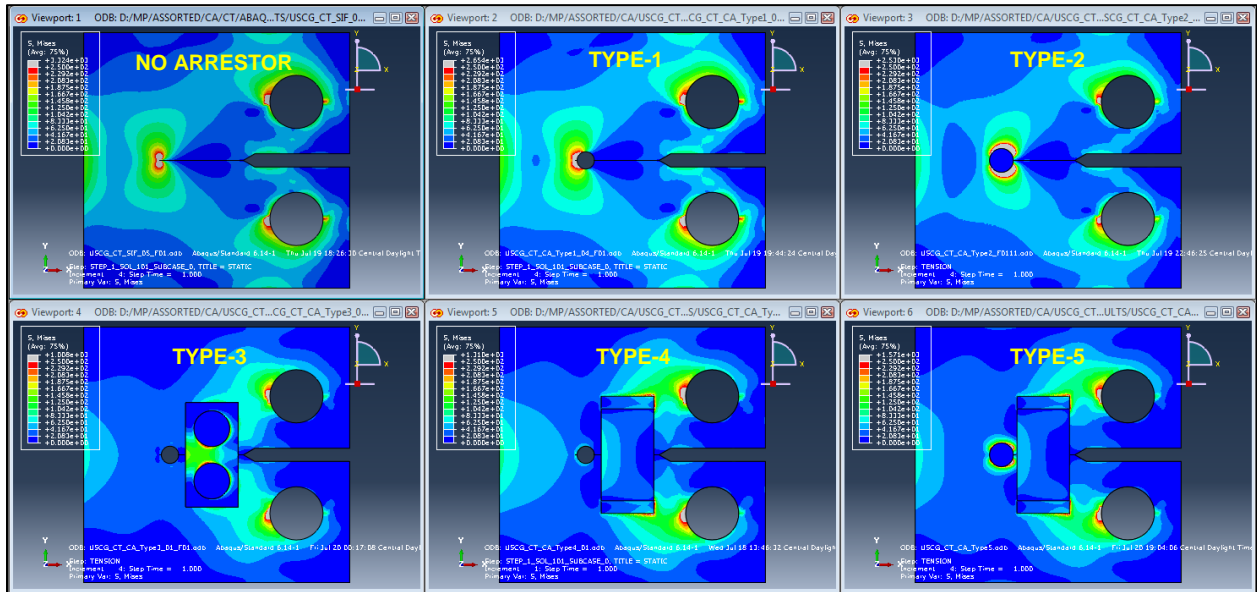


Figure 5-8: Von Mises Stress Contour for Different Crack Arrestors

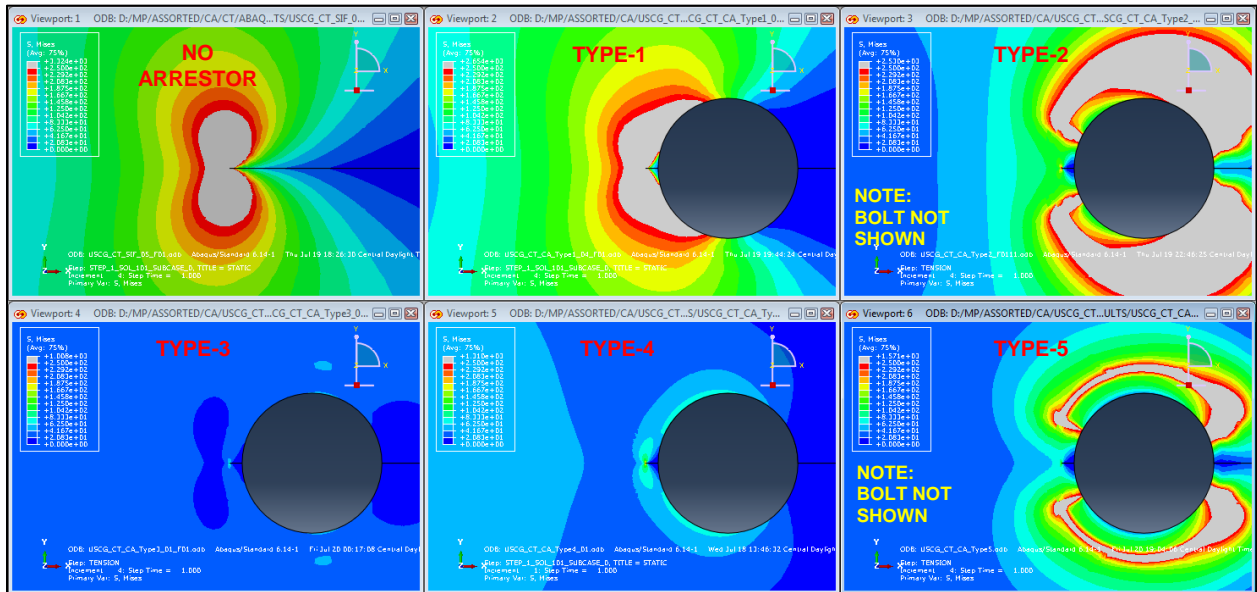


Figure 5-9: Von Mises Stress Contour Focused at the Crack Tip Region

5.7 Performance Evaluation

5.7.1 Performance Evaluation Based on the Stress Intensity Factor (SIF)

Figure 5-10 below is a simple demonstration of the performance of different arrestor types evaluated based on the stress intensity factors (SIF's). Please note that in all the SIF's computed below for the specimen are at the constant crack length of 1.6 inch (40 mm). The thickness of the specimen is 8mm and the chart below represents the SIF's at every unit mm of the depth of the specimen (surface to surface).

The graphical representation in Figure 5-10 below, infers that just with an inclusion of a crack arrestor hole (CAH) at the crack tip, the stress intensity is considerably reduced. Further as we introduce different arrestors in addition to a CAH, the stress Intensity Factors (SIF) approaching the critical ($K_{Ic} \sim 44 \text{ Mpa}\sqrt{\text{m}}$) can be shifted towards the threshold value of the material ($K_{th} \sim 3 \text{ Mpa}\sqrt{\text{m}}$), thus reducing the crack growth rate and achieving improved fatigue performance.

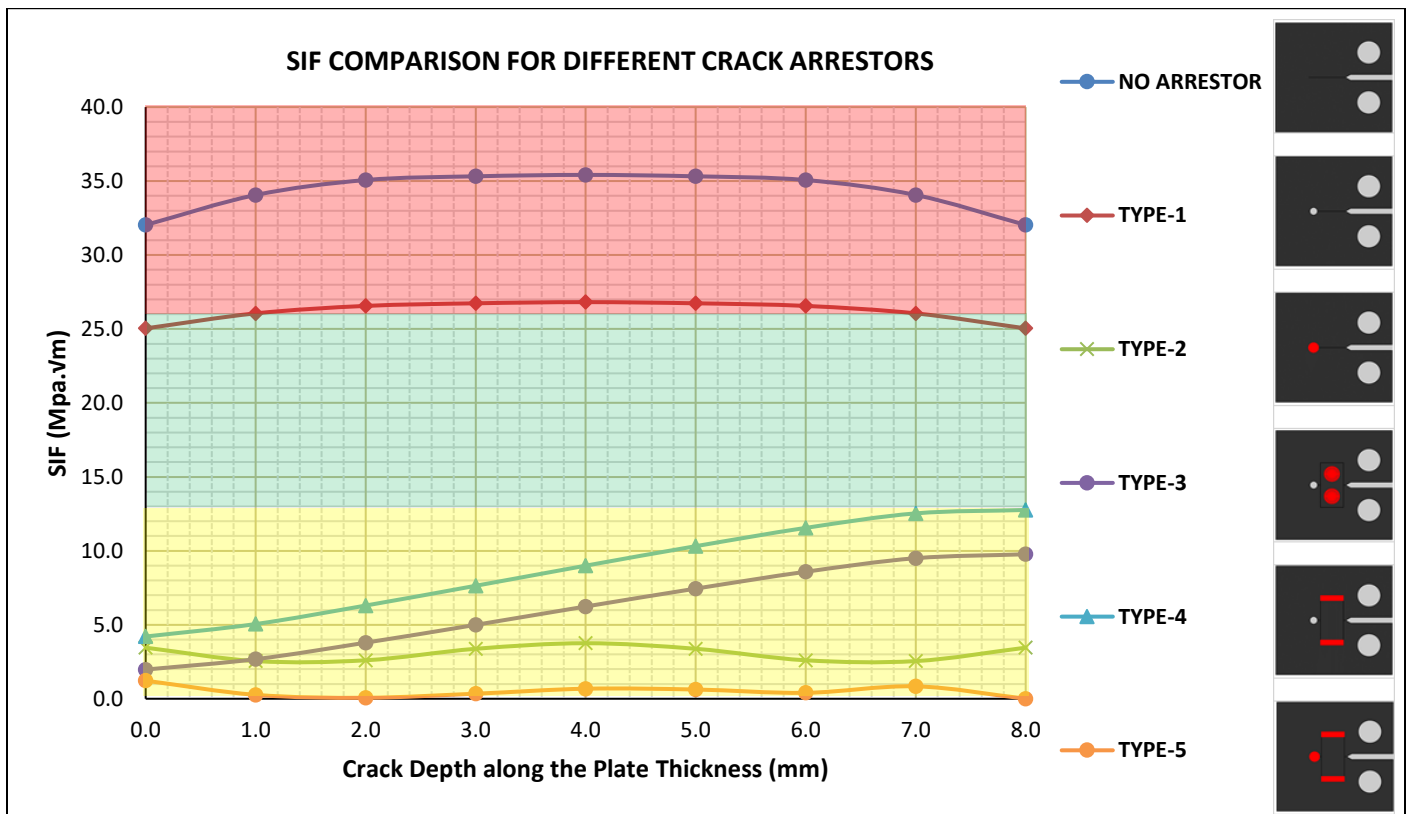


Figure 5-10: SIF Comparison for Different Crack Arrestor Types

5.7.2 Performance Evaluation Based on the Endurance to Cyclic Loading

This section demonstrates the performance of different arrestors based on their endurance to Cyclic Fatigue Loads. A low cyclic fatigue load under a constant, conservative amplitude was applied to each specimen with different arrestors. The crack growth was then monitored implementing the XFEM (Extended Finite Element Method) in Abaqus, as shown in Figure 5-11 below.

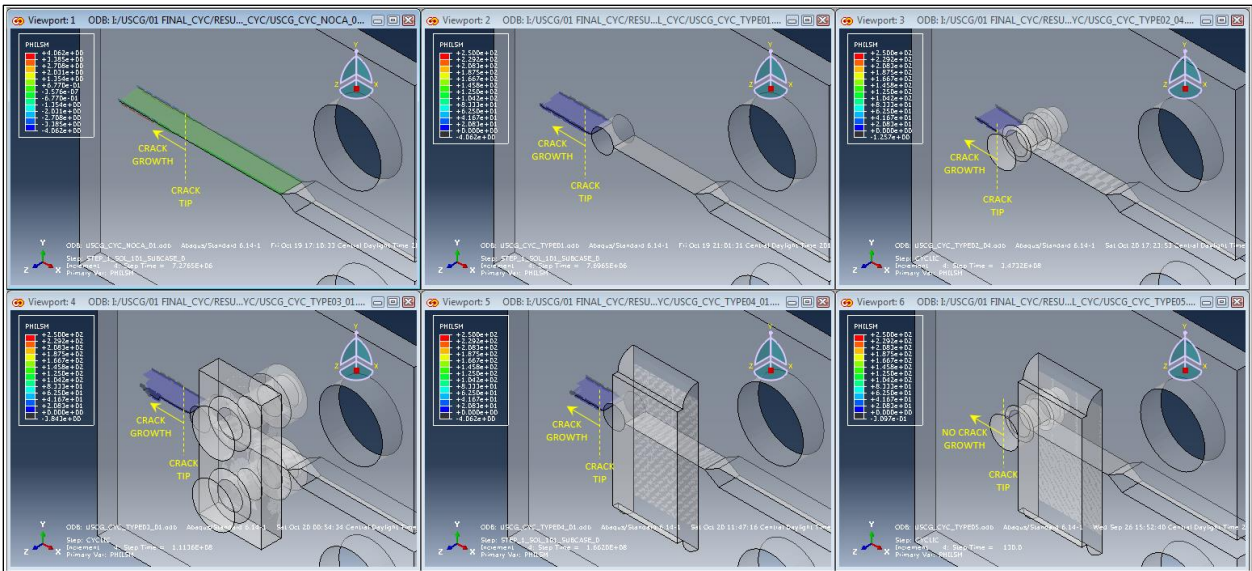
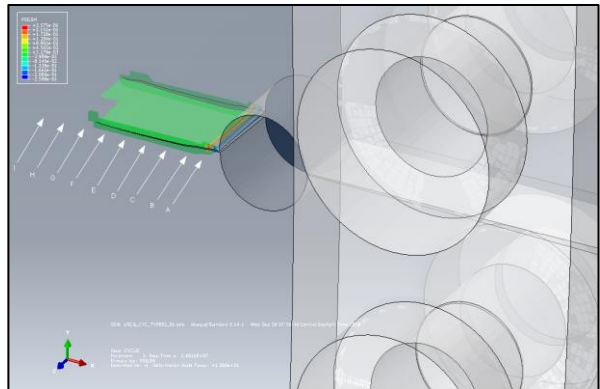
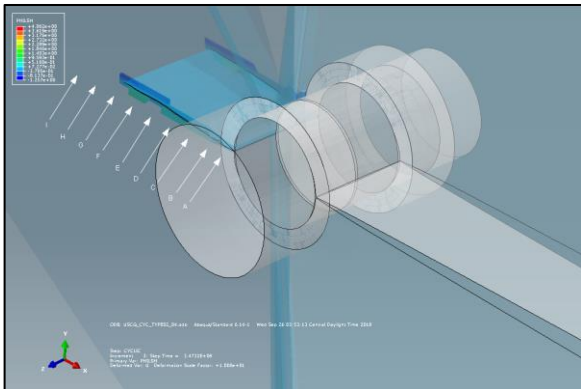
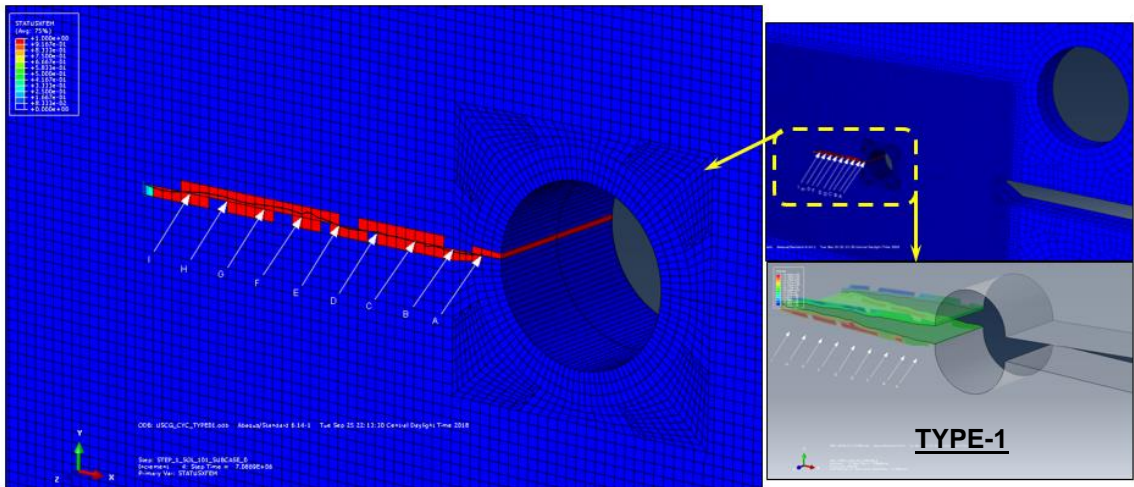
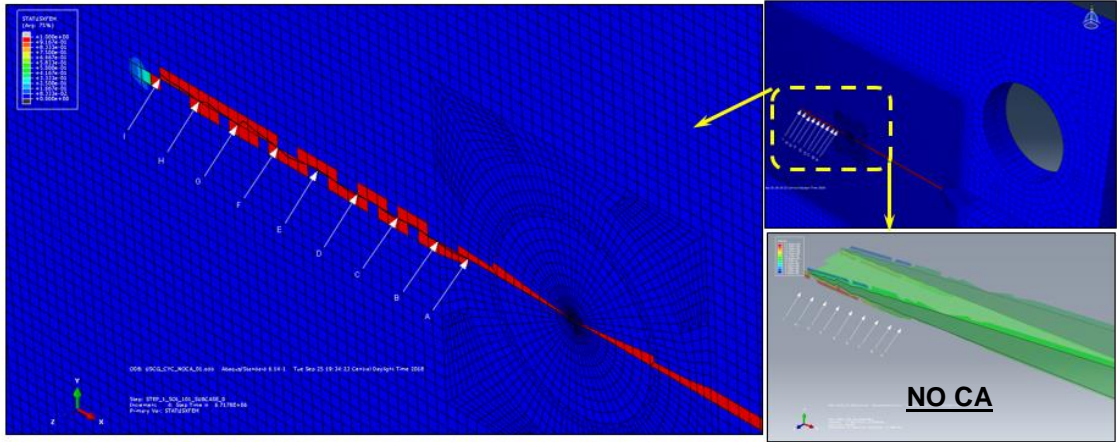


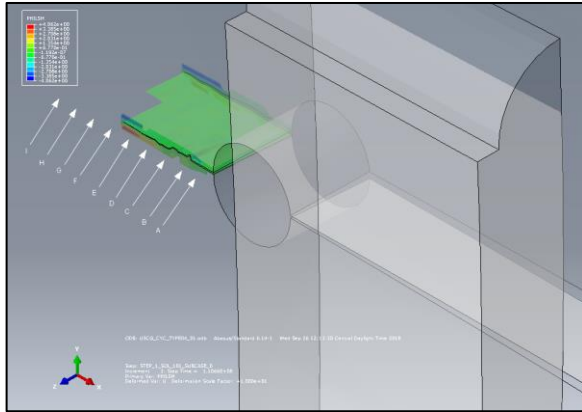
Figure 5-11: Performance under Cyclic Loading for Different Arrestors

Figure 5-12 shows the data points set up to monitor the rate of crack growth.

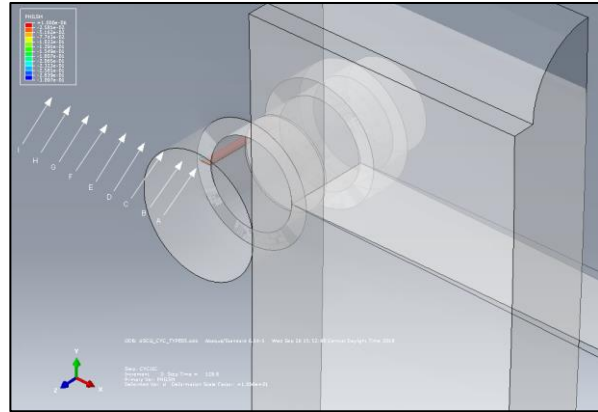
Table 5-2 below compares the 'Number of Cycles' for each increment in the crack length that was monitored at different set of data points.

The statistics clearly infers that there is a significant reduction in the crack growth rate after introduction of different arrestors to the original specimen with crack.





TYPE-4



TYPE-5

Figure 5-12: Performance under Cyclic Loading for Different Arrestors (Monitoring Points)

Table 5-2 : Statistics of Crack Growth Rate for Different Crack Arrestor Types

DATA POINTS Label	CRACK LENGTH a (mm)	(NO OF CYCLES) FOR DIFFERENT ATTESTOR TYPES					
		NO CA	TYPE 1	TYPE 2	TYPE 3	TYPE 4	TYPE 5
A	40	0	0	0	0	0	0
B	41.5	6.67E+04	2.07E+05	4.39E+07	2.15E+06	2.18E+06	NO GROWTH
C	43.5	9.60E+05	3.25E+06	6.31E+07	3.36E+06	2.33E+07	
D	45.5	3.39E+06	3.39E+06	8.79E+07	5.28E+06	2.62E+07	
E	47.5	3.50E+06	3.53E+06	1.07E+08	7.19E+06	8.20E+07	
F	49.5	3.84E+06	4.89E+06	2.29E+08	8.04E+06	1.08E+08	
G	51.5	4.63E+06	5.50E+06	3.47E+08	2.48E+07	1.11E+08	
H	53.5	5.32E+06	5.88E+06	NOT MONITORED			
I	55.5	6.65E+06	6.90E+06				
Average CGR (da/dN) ->		7.13E-06	6.13E-06	5.91E-08	1.15E-06	3.78E-07	0.00E+00

6 Trade-off Study

The above studied arrestors on the CT specimen were introduced into the local crack propagation ship model at the two (2) previously selected locations critical for bending and slamming, subject to multiaxial loadings in the subsequent section.

6.1 Application of Crack Arrestors – Midship Section

Figure 6-1 below represents the introduction of previously studied crack arrestors in the local crack propagation models for the midship section. The method of evaluation of the crack arrestor is analogous to the one explained in Section-5, except that the loading condition relates to the stress field obtained from the global analysis.

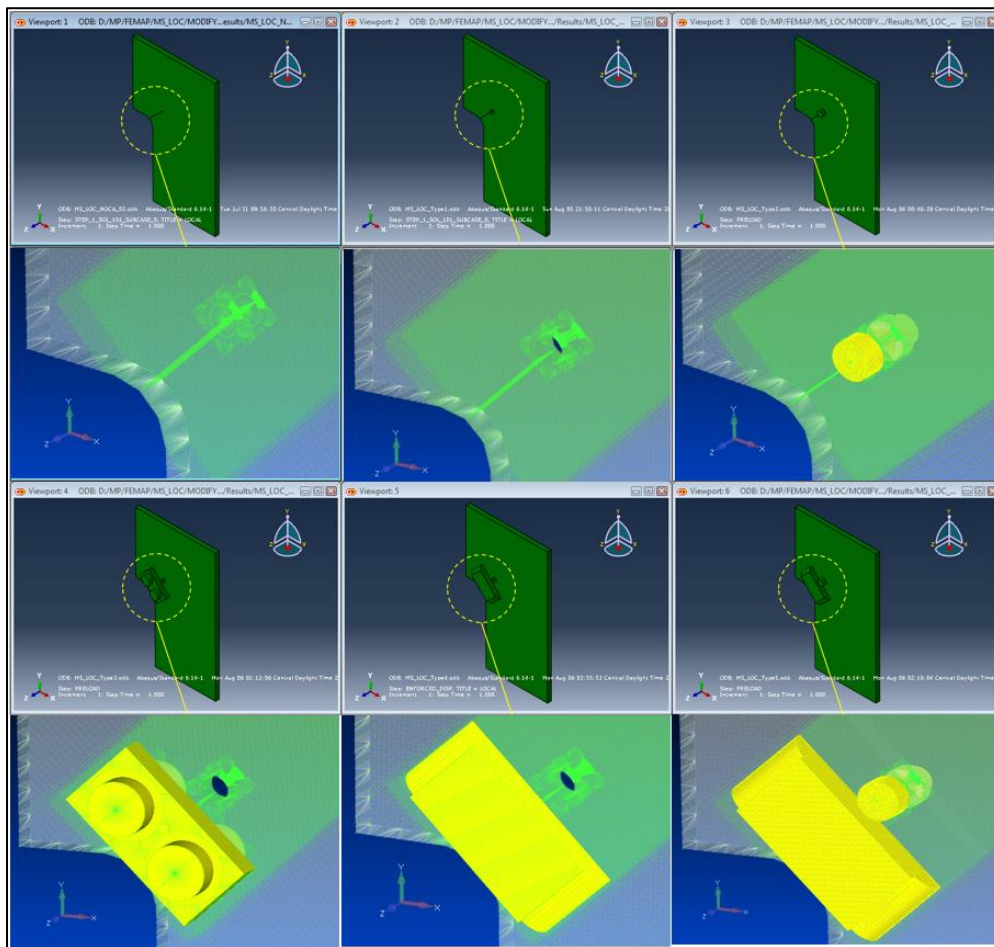


Figure 6-1: Introduction of different Crack Arrestors – Midship Section

Figure 6-2 below represents the von Mises stress contour for different studied crack arrestors at the selected critical midship location, whereas Figure 6-3 below represents the stress contour at the crack tip region showing the variation in the magnitude of plastic zone at the crack tip region with the introduction of different crack arrestors.

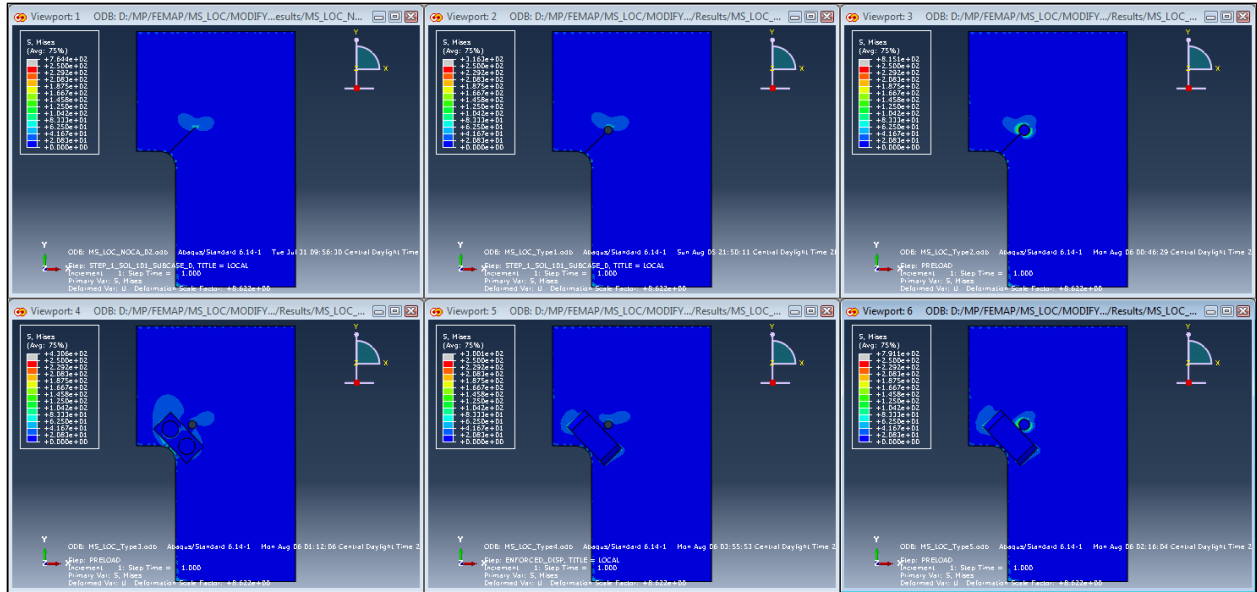


Figure 6-2: Von Mises Stress Contour Focused at the Crack Tip Region – Midship Section

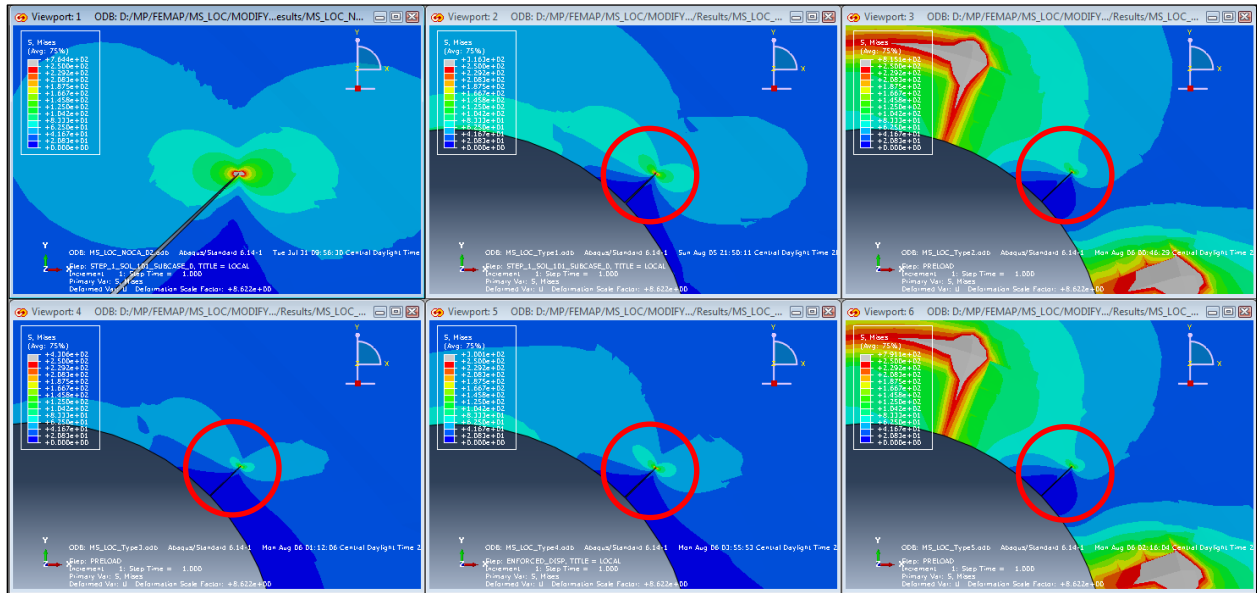


Figure 6-3: Von Mises Stress Contour Focused at the Crack Tip Region– Midship Section

Figure 6-4 below compares the SIF's for different crack arrestor types at the critical midship section, which demonstrates the reduction in stress intensity factors after introduction of the crack arrestors.

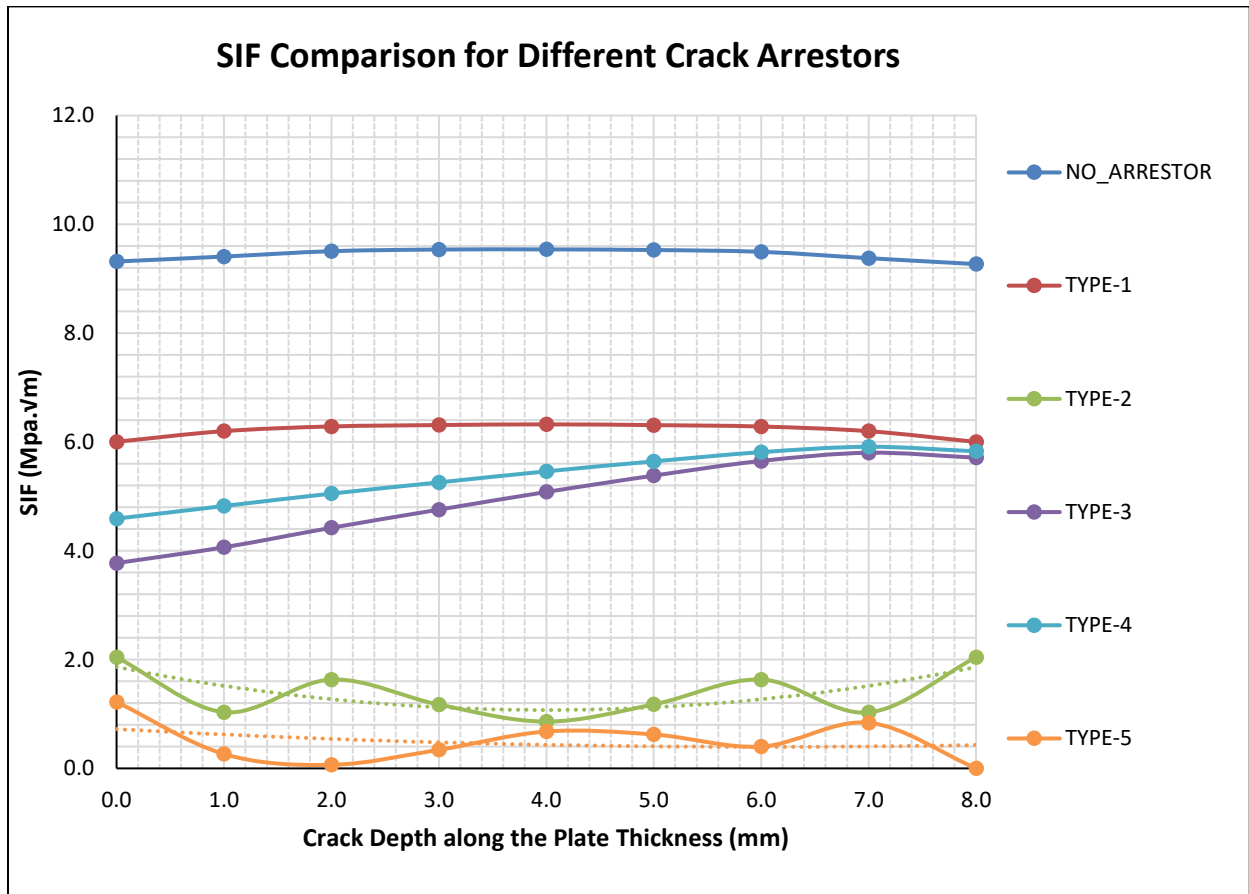


Figure 6-4: SIF Comparison for Different Crack Arrestor Types – Midship Section

6.2 Application of Crack Arrestors – Bow Section

Figure 6-5 below represents the introduction of previously studied crack arrestors (Type-1 & Type-2) in the local crack propagation models for the critical bow section. The method of evaluation of the crack arrestor is analogous to the one explained in Section-5, except that the loading condition relates to the stress field obtained from the global analysis.

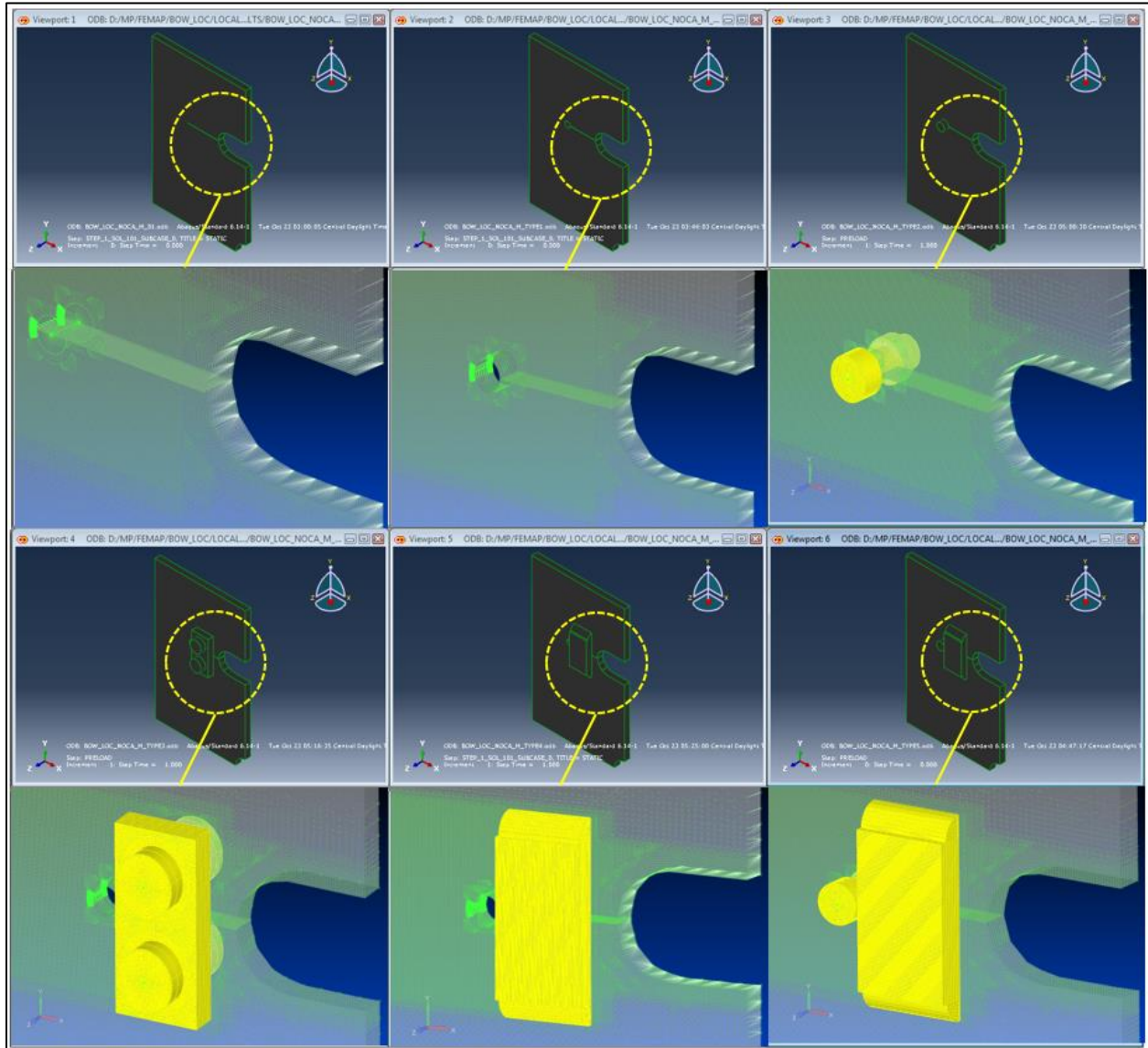


Figure 6-5: Introduction of different Crack Arrestors – Bow Section

Figure 6-6 below represents the von Mises stress contour for different studied crack arrestors at the selected critical bow location, whereas Figure 6-7 below represents the stress contour at the crack tip region showing the variation in the magnitude of plastic zone at the crack tip region with the introduction of different crack arrestors.

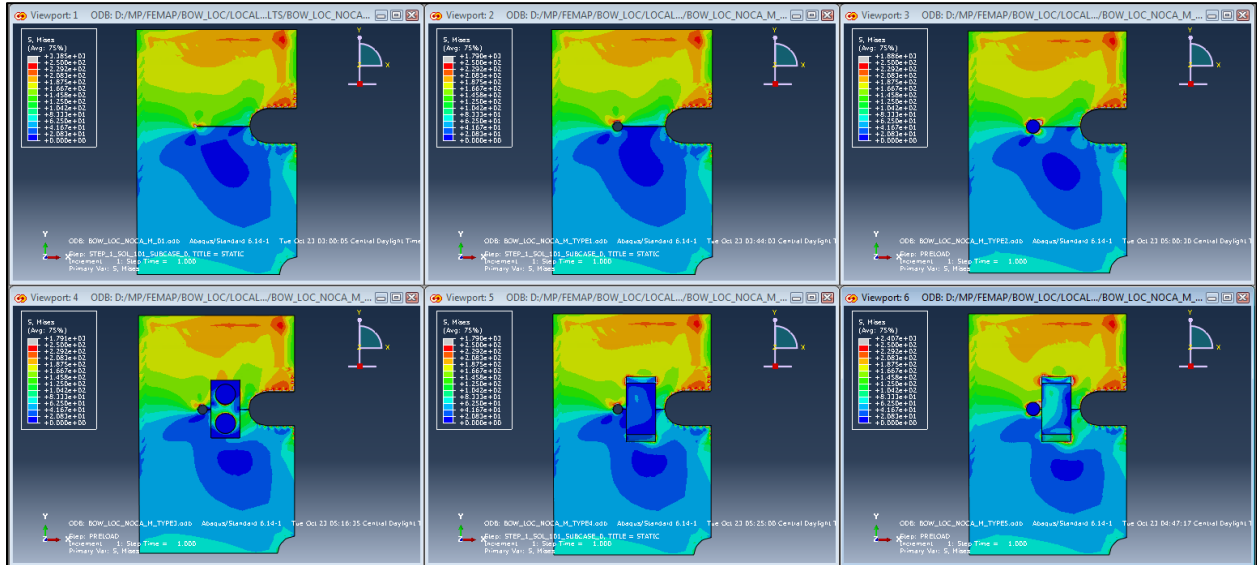


Figure 6-6: Von Mises Stress Contour for Different Crack Arrestors – Bow Section

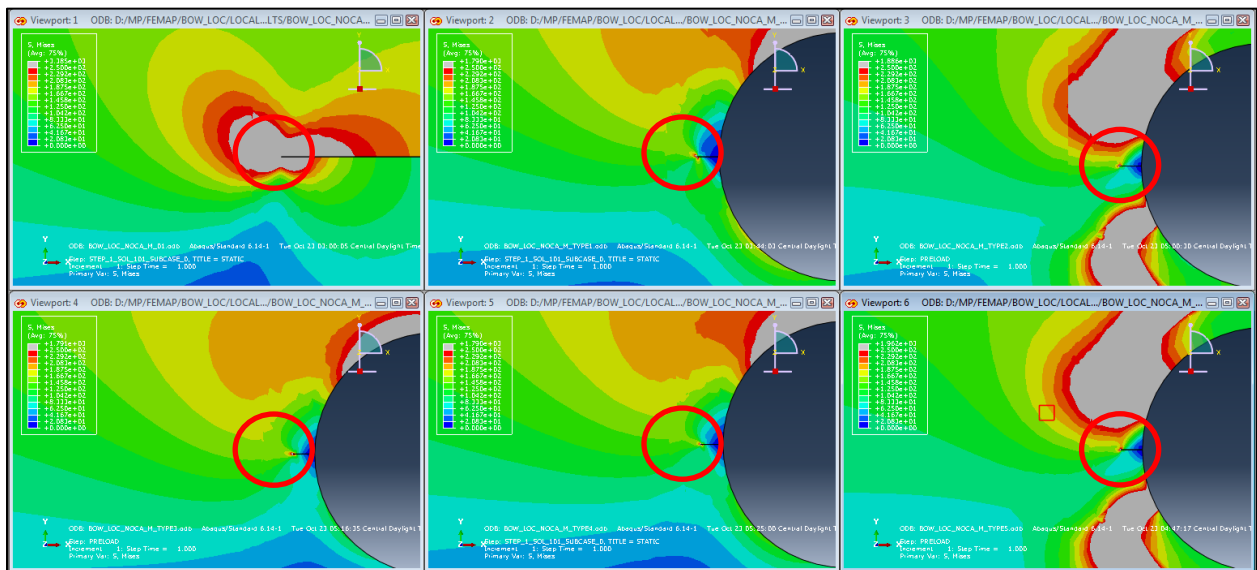


Figure 6-7: Von Mises Stress Contour Focused at the Crack Tip Region – Bow Section

Figure 6-8 below compares the SIF's for different crack arrestor types at the critical bow section, which infers the reduction in stress intensity factors after introduction of the crack arrestors.

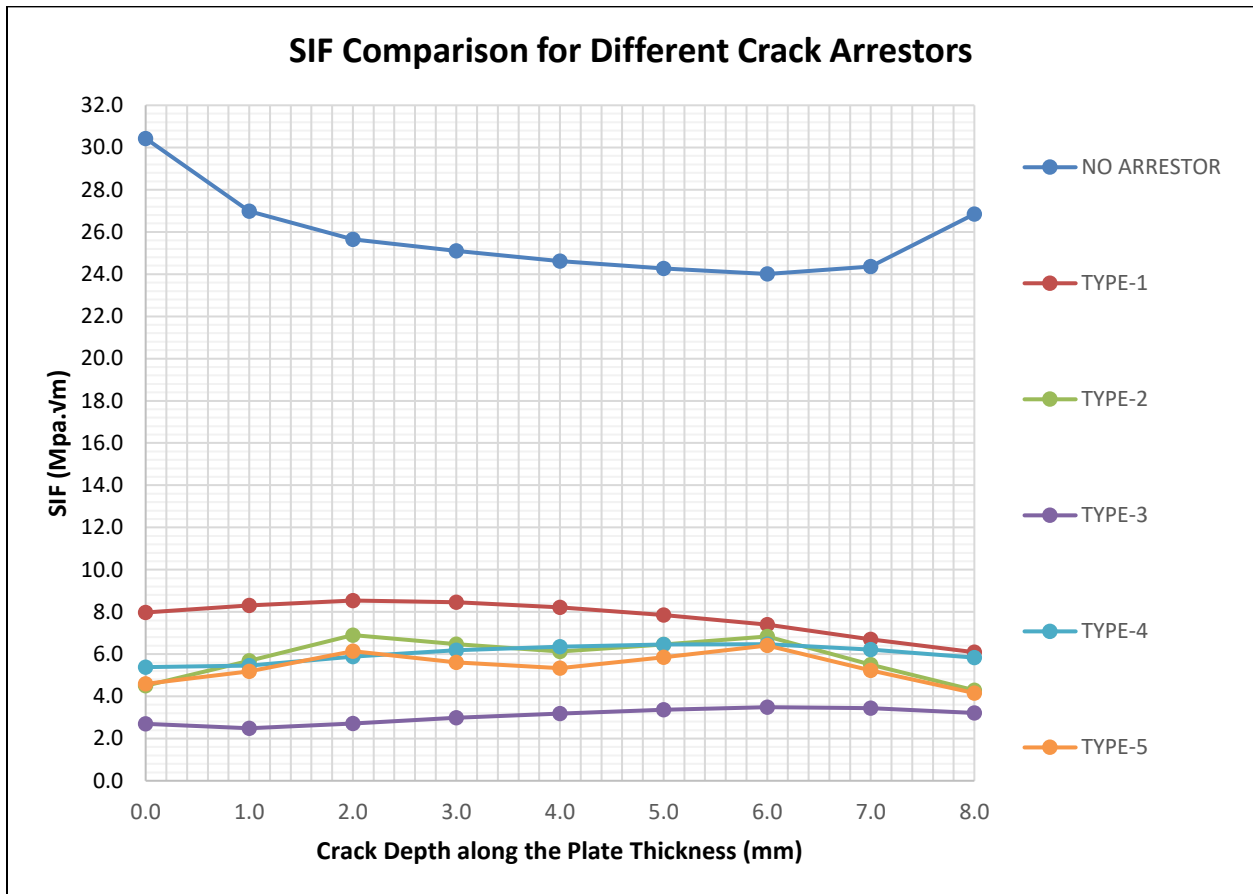


Figure 6-8: SIF Comparison for Different Crack Arrestor Types – Bow Section

6.3 Guidance on Selection of Crack Arrestor

The following are some brief guidance notes on the selection, use and proposed modifications/improvements to the studied crack arrestor types:

- **TYPE-1 - CAH (Crack Arrest Hole)**

This is the simplest and commonly used arrestor type currently being employed in the industry. Though some instances, based on the industry experience, have shown that the crack continues to grow after introduction of a CAH, this arrestor still can offer sufficient timeframe to the operator/or designer to plan and execute a more permanent repair (if warranted).

The diameter of the CAH (Crack Arrest Hole) needs to be at least the thickness of the plate with defect (OR as warranted by the interference bolt, if the corresponding arrestor is selected for use).

- **TYPE-2 - CAH (Crack Arrest Hole) with Interference Bolt**

Applicable scenarios for the use of arrestor type-2 i.e. CAH (Crack Arrest Hole) with interference bolt:

- When the length of observed crack is up to 25mm (1”), however, can also be used for higher crack lengths.
- When there are restrictions on the execution of repairs involving ‘hot work’ without halt in the normal operations.

The Interference Bolts are secured with the washer and nuts on the other end of the plate and shall meet a minimum of ASTM A325 grade or higher, which is widely used in the industry for various structural connections. The bolt preload to be applied is determined in such a manner that, the resultant stresses due to the preload is either equal to or less than the yield strength of the plate being repaired.

- **TYPE-3 - CAH (Crack Arrest Hole) with Bolted Patch Plate**

Applicable scenarios for use of arrestor type-3 i.e. CAH (Crack Arrest Hole) with bolted patch plate:

- When the length of observed crack varies between 30mm to 50mm (1.25” – 2”).
- When there are restrictions on the execution of repairs involving ‘hot work’ without halt in the normal process / operations.

Due to the presence of patch plate only on one side, the nature of SIF curve for Type-3 under Figure 5-10 suggest that the SIF tends to increase on the opposite end. Hence, arrestor TYPE-3A can be introduced, as shown in Figure 6-9 , that will contain a sandwich plate on the rear end of the plate. This suggested arrestor type

could not be studied computationally in the current study, hence added as an item for future work. The bolt preload to be applied is determined in such a manner that, the resultant stresses due to the preload is either equal to or less than the yield strength of the plate being repaired.

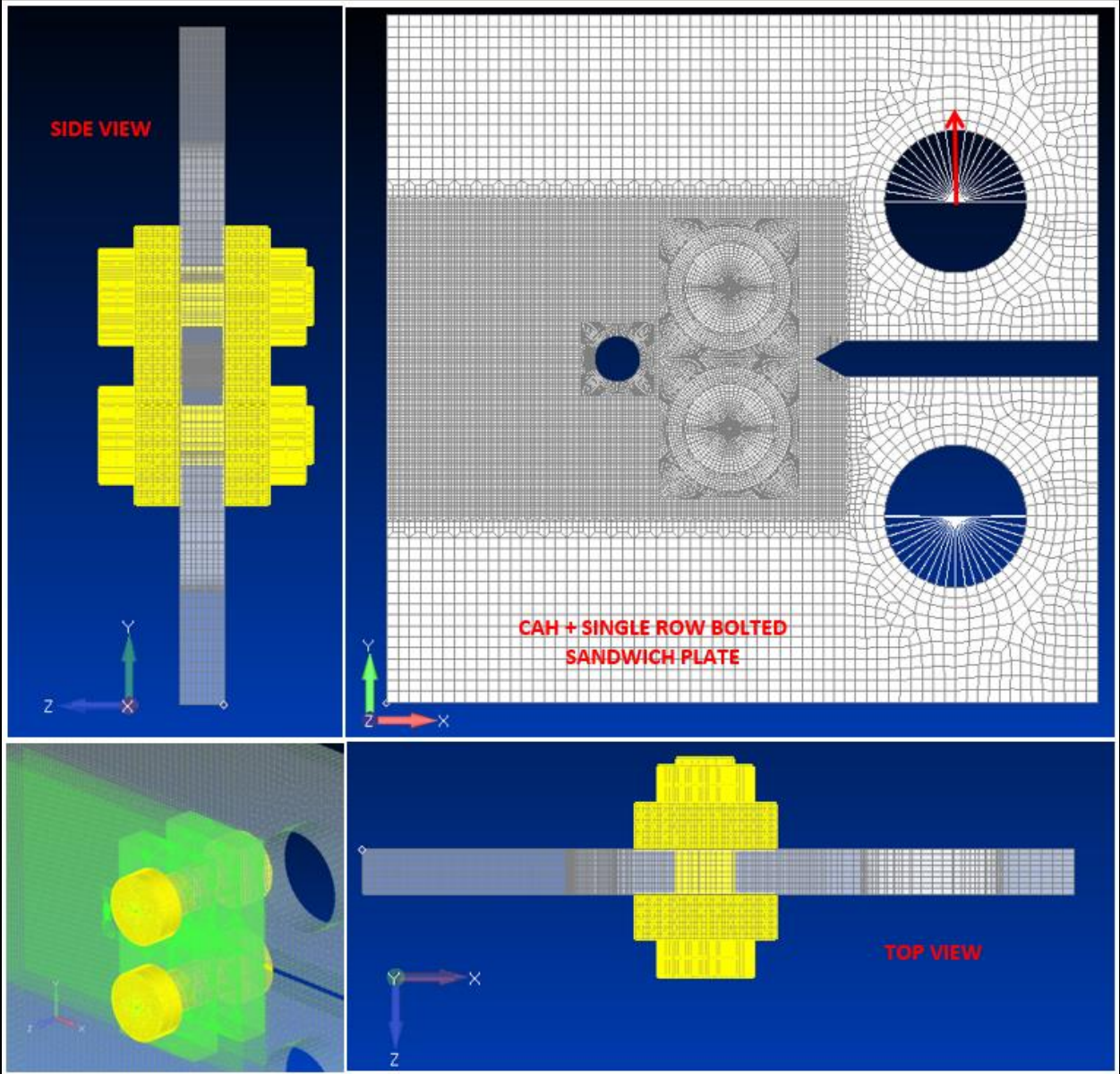


Figure 6-9: CRACK ARRESTOR TYPE-3A - CAH (Crack Arrest Hole) with Single Row Bolted Patch Plate

Following additional modification to the type-3, as shown in Figure 6-10 below, will allow effective application of type-3 arrestors to for higher crack lengths beyond 50mm.

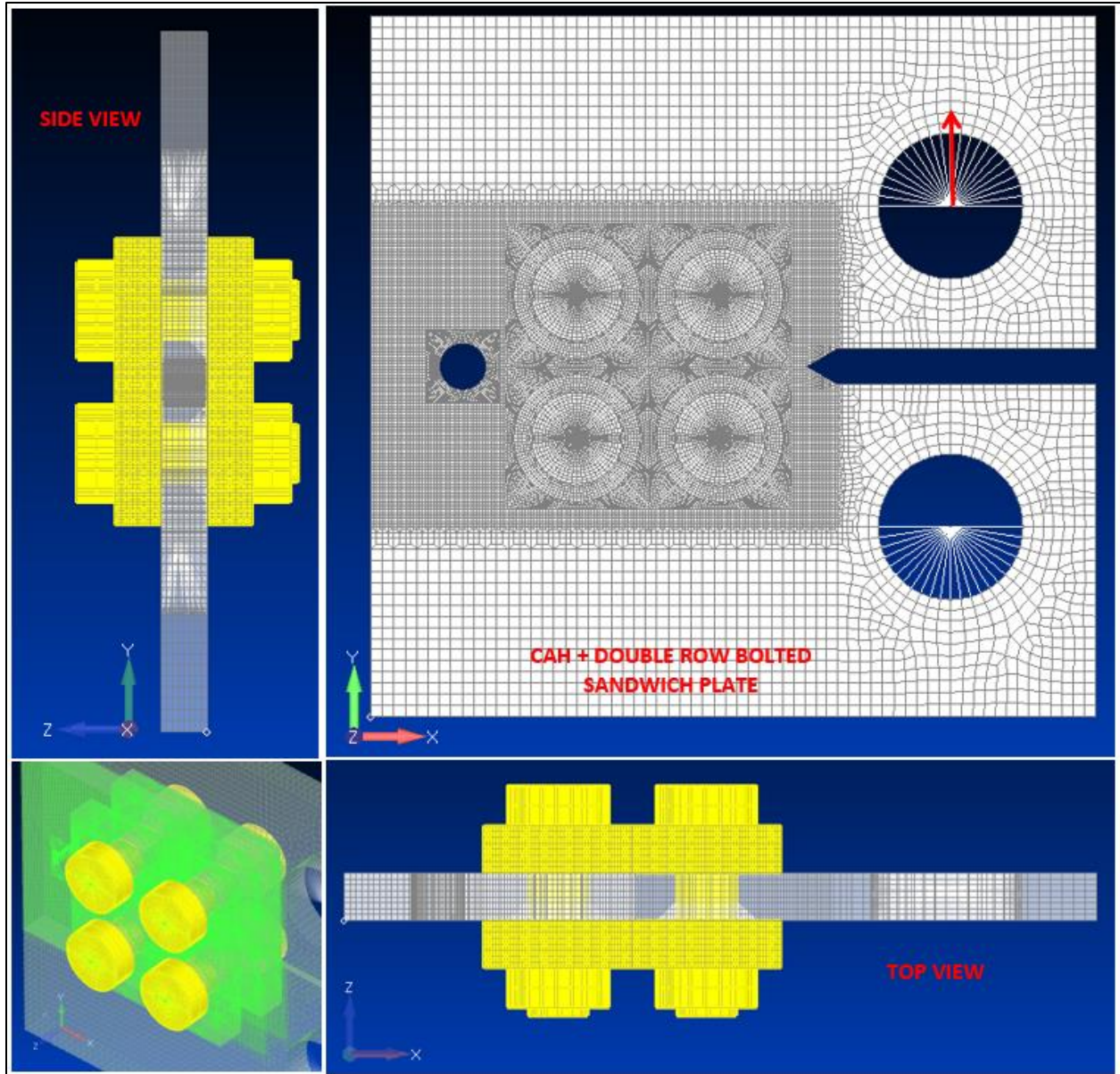


Figure 6-10: CRACK ARRESTOR TYPE-3B - CAH (Crack Arrest Hole) with Double Row Bolted Patch Plate

- **TYPE-4 - CAH (Crack Arrest Hole) with Welded Patch Plate**

Applicable scenarios for use of arrestor type-4 i.e. CAH (Crack Arrest Hole) with welded patch plate:

- When the length of observed crack varies between 30mm to 50mm (1.25" – 2").
- When there are NO restrictions on the execution of repairs involving ‘hot work’

The following modification to the type-4, as shown in Figure 6-11 below, will allow effective extension to the application of type-4 arrestors for higher crack lengths beyond 50mm lengths. This arrestor can also be categorized as a permanent repair method.

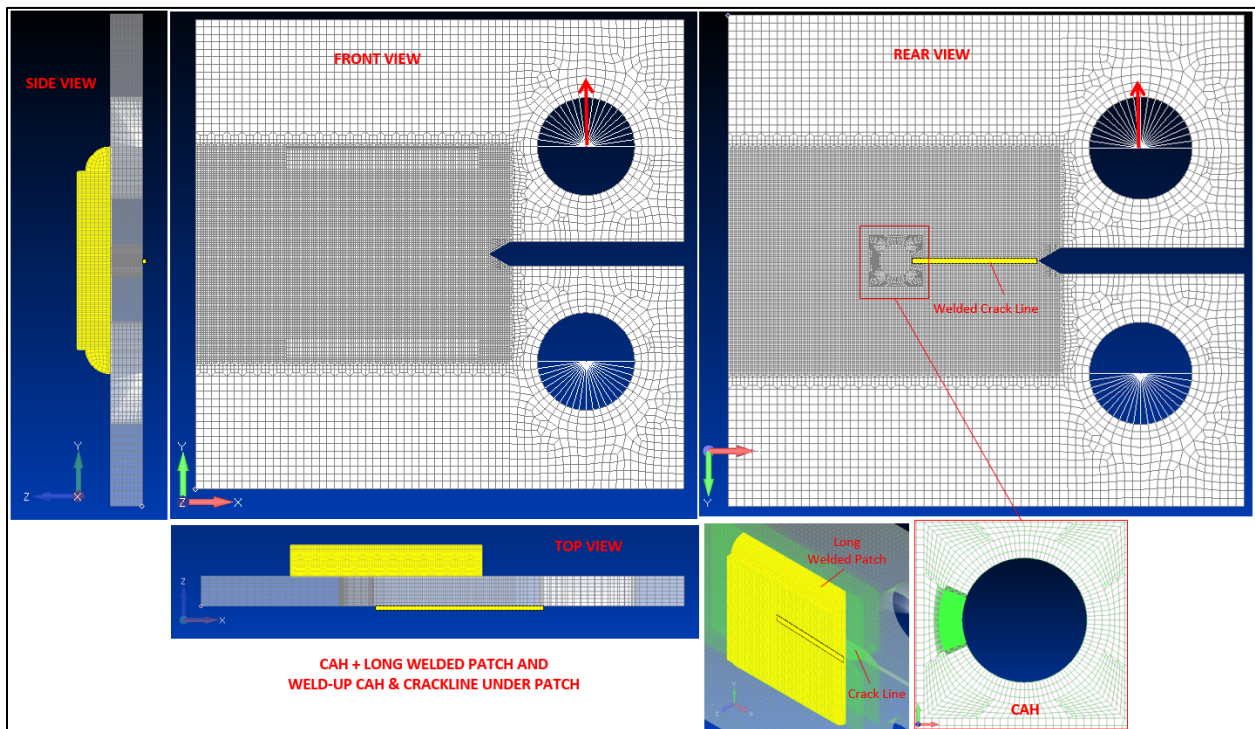


Figure 6-11: CRACK ARRESTOR TYPE-4A - CAH (Crack Arrest Hole) with Long Bolted Patch and Weld-up CAH & Crack Line under Patch

- **TYPE-5 - CAH (Crack Arrest Hole) with Interference Bolt & Welded Patch Plate**

This arrestor is a combination of Type-2 and Type-4. This arrestor, type-5, was included in study since arrestor Type-4 alone presented lower performance when compared to Type-2 & Type-3.

Thus, the applicable scenarios for use of arrestor type-5 i.e. CAH (Crack Arrest Hole) with interference bolt & welded patch plate:

- When the length of observed crack varies between 30mm to 50mm (1.25" – 2").
- When there are restrictions on the execution of repairs involving 'hot work' without halt in the normal operations.

This arrestor also showed promising results (refer Section 5.7.1 and 5.7.2) to completely eliminate the further crack growth even under the presence of a test slit (0.5mm) that was introduced in all other arrestor types. The bolt preload to be applied is determined in such a manner that, the resultant stresses due to the preload is either equal to or less than the yield strength of the plate being repaired.

7 Discussion and Concluding Remarks

ABS Consulting Inc. (ABSG) has been tasked by the SSC through the USCG to develop and verify a design and performance evaluation method for crack arrestor enhanced aluminum marine structures.

In order to meet the project objectives, following five (5) distinct tasks were performed:

- *Task 1: Literature Review*
- *Task 2: Modeling and Prediction of Crack Initiation and Growth*
- *Task 3: Perform a Tradeoff Study*
- *Task 4: Modeling Verification & Validation*
- *Task 5: Technical Report Writing*

ABS Consulting studied performance of five (5) different types of crack arrestors and they are discussed in detail under Section 5 of this report.

This report summarizes the work performed under the above-mentioned tasks, the results obtained, and provides a detailed explanation of the methodology used to meet the project objectives.

The following recommendations are proposed:

- All the studied models are recommended to be tested in lab to revalidate the results and so that necessary calibration can be done.
- The proposed crack arrestors shall be considered “temporary repair”, but not the “permanent repair” (with an exception to type-4A), and it is recommended that the repaired locations are re-inspected / monitored periodically no more than an annual interval, until the permanent repairs (if warranted) are executed.
- Recommended to study additional modifications to the studied Crack Arrestors as follows those are addressed in Section 6.3:
 - TYPE-3A - CAH (Crack Arrest Hole) with Single Row Bolted Patch Plate
 - TYPE-3B - CAH (Crack Arrest Hole) with Double Row Bolted Patch Plate
 - TYPE-4A - CAH (Crack Arrest Hole) with Long Bolted Patch and Weld-up CAH & Crack Line under Patch

Following are the potential areas/topics for future work that shall be considered and integrated while implementing the proposed arrestor’s types:

- Extension of Arrestors to Curvilinear Cracks
- Consideration of Welding Induced Stresses
- Study of additional types of arrestors (Recommended in Section 6.3)
- Evaluating the performance of arrestors without a slit at the crack tip
- Welding Induced Material Heterogeneity
- Stress-corrosion cracking and material sensitization

8 References

A list of the articles that ABS Consulting has collected and reviewed during the course of project are summarized in **Appendix – B**.

APPENDIX A. Reference Drawings for Vessel

Note: Reference drawings exist in alternate file form. Drawings will be included in published version.

APPENDIX B. Literature Review

A list of the articles that ABS Consulting has collected and reviewed during the course of project are summarized in below:

1. Galanis K.P., Papazoglou V.J. (2007) Crack Propagation in Naval Aluminum Panels. In: Gdoutos E.E. (eds) Experimental Analysis of Nano and Engineering Materials and Structures. Springer, Dordrecht

A ship structure can be regarded as a complex assemblage of continuous stiffened plates. The most common mode of failure of such plates is fracture. Crack propagation and arrest in naval aluminum panels, however, has not been an area of in-depth research. As a consequence, the increased use of aluminum in the shipbuilding industry is highly dependent on the understanding of the fracture mechanics that govern naval aluminum panels, given that the vessels operate in extreme environmental and functional conditions that may lead to the loss of the entire structure.

2. Frandsen, J.D., Fatigue Crack Growth in Aluminum Alloys, Final Report, Rockwell International Thousand Oaks California Science Center, 27 February 1976. DTIC Accession Number: ADA025196.

The objective of this investigation was to further the understanding of the mechanisms by which fatigue crack propagation occurs in aluminum alloys. Two basic techniques were used to investigate and simulate the events occurring within the plastic zone preceding fracture. The plastic deformation occurring within the plastic zone of the crack tip was simulated by low cycle fatigue tests. These tests were largely unsuccessful because of the significant influence the crack initiation stage has on fatigue life and a relative insensitivity to environmental effects. The response of the crack tip to tensile holds was determined by acoustically determined crack closure measurements. The limited results reported here were encouraging and the crack closure investigation offers possibilities of describing the fatigue cracks response to simple loading spectra.

3. Irwin, G.R., NRL Report 4763: Onset of Fast Crack Propagation in High Strength Steel and Aluminum Alloys, Naval Research Laboratory Mechanics Division, Washington D.C., May 24, 1956.

The concept of driving force per unit crack front or the “force tendency” is discussed. This is a more general and more readily useful concept than the Griffith theory in that it does not require the assumption of the absence of plasticity and there is no complication involving fixed grips. It is shown that the force tendency exists for any stress condition and that it can be determined for strain measurements near the crack head. Various

formula for the force tendency is given and the case of hydrogen embrittlement is discussed.

4. Lee, O.S., Kim, D.Y., Crack-Arrest Phenomenon of an Aluminum Alloy, Mechanics Research Communications, Volume 26, No. 5, pp. 575-581, Elsevier Science Ltd., 1999.

Engineering failures may be defined as the structural states which are unsuitable to accomplish the design purposes of the structure. A significant structural failure is known to be frequently caused by the crack. Therefore, studies on the crack-initiation and crack-propagation are very important to prevent structural failure. However, the crack-initiation is inevitable in many cases, and thus the crack-arrest capability of the structural materials is known to be a significant material property to assess the integrity of the structural components. The crack-arrest capability can be quantified by crack-arrest toughness, which is considered as the ability of material to stop a fast running crack. The ASTM published "Standard Test Method for Determining Plane-Strain Crack-Arrest Fracture Toughness, K_{Ic} , of Ferritic Steels", which is basically for nuclear ferritic steels. The main goal of this research is to examine whether the ASTM standard can be applied to an aluminum alloy such as A1 5083 H-112 which is used for fast-sailing boats and offshore structures. A review of crack-arrest fracture testing is also provided in this study.

5. Murdani, A. et. al., A Crack-Growth Arresting Technique in Aluminum Alloy, Engineering Failure Analysis, Volume 15, Issue 4, pp. 302-310, Elsevier Science Ltd., June 2008.

The purpose of the present study is to propose a new technical method for arresting crack initiation at stop-drilled holes by drilling ancillary holes following the making of the stop-drilled holes. The main idea of the method is to reduce the stress concentration at the edges of stop-drilled holes. To confirm the effectiveness of the method, analyses were performed by using software for two-dimensional elastic problems based on the body-force method, and some experiments were carried out. The calculation results show that the existence of ancillary holes effectively reduced the stress concentration at the edges of the stop-drilled holes. A close distance between the stop-drilled hole and the ancillary holes resulted in lower stress concentration at the edge of the stop-drilled hole. Also, a considerable reduction of stress concentration was obtained by arranging for the diameter of the ancillary holes to be larger than that of the stop-drilled holes. Consecutively, the experimental results showed that the fatigue initiation life was in good agreement with the calculation results.

6. Khelil, F. et. al., Modeling of Fatigue Crack Propagation in Aluminum Alloys Using an Energy Based Approach, ETASR – Engineering, Technology & Applied Science Research, Vol. 3, No. 4, pp. 488-496, 2013.

Materials fatigue is a particularly serious and unsafe kind of material destruction. Investigations of the fatigue crack growth rate and fatigue life constitute very important

and complex problems in mechanics. The understanding of the cracking mechanisms, taking into account various factors such as the load pattern, the strain rate, the stress ratio, etc., is of a first need. In this work an energy approach of the Fatigue Crack Growth (FCG) was proposed. This approach is based on the numerical determination of the plastic zone by introducing a novel form of plastic radius. The experimental results conducted on two aluminum alloys of types 2024-T351 and 7075-T7351 were exploited to validate the developed numerical model. A good agreement has been found between the two types of results.

7. Hahn, G.T., Simon, R., Metallurgical Control of Fatigue Crack Growth in High-Strength Aluminum Alloys, Air Force Materials Laboratory Technical Report AFML-TR-72-48, May 1972.

The results of 22 different investigations of cyclic crack growth, principally on the 2024-T3 and 7075-T6 alloys, but including results for unalloyed and other 2-, 5-, 6-, and 7-thousand series alloys have been examined and compiled with a view to separating metallurgical effects from other factors. The various crack growth measurements show good agreement when the comparisons involve the same R-value, environment and cyclic frequency. Both the 2024-T3 and 7075-T6 alloy can display widely different rates of growth for the same ΔK -value. The highest growth rates are for tests in humid air, the lowest growth rates for tests in dehydrated air with high cyclic frequencies. These extremes point to a moisture assisted corrosion process capable of producing a 20-fold increase in the growth rate at low ΔK -levels.

Crack growth rate- ΔK measurements have also been converted into S-N curves for cracked members. These curves illustrate the influence of flaw size, stress range, R and K_{IC} on the cyclic life of the 7075-T6 and 2024-T3 grades. The S-N curves show that the cyclic life of 2024-T3 is about 3x that of 7075-T6 in laboratory air, about 5x that of 7075-T6 in humidified air, and 10x that of 7075-T6 if ΔK is in proportion to the yield strength. Finally, recent studies of the mechanisms of cyclic growth and other observations bearing on the contribution of metallurgical factors are examined. Effects associated with composition, heat treatment, small amounts of cold work, hard particles and inclusions, grain boundaries, the dislocation substructure produced by cyclic straining, and slip offsets are discussed.

8. Wei, R.P. Fatigue-crack propagation in a high-strength aluminum alloy, Int J Fract (1968) 4: 159.

Fatigue-crack propagation experiments were carried out within the framework of linear-elastic fracture mechanics to examine the effect of water and its constituents on the rate of crack growth in a high-strength aluminum alloy over a range of test temperatures from 295 to 380° K. Dehumidified high-purity (99.9995 percent purity) argon was used as an inert reference environment. The results showed that water accelerated the rate of fatigue-crack propagation by about a factor of 10 in this temperature range, whereas dry

oxygen and dry hydrogen had a negligible effect. They confirm the findings of Hartman, and Bradshaw and Wheeler that the cause for the large increase in the rate of crack growth is the formation of hydrogen gas at high pressure in the region ahead of the crack tip, driven in by the reaction of water with the-freshly created aluminum crack surfaces, as suggested by Broom and Nicholson. The results showed further that fatigue-crack propagation in water, as well as in the dry environments, is controlled by thermally activated processes, with apparent activation energies that depend strongly on the crack-tip stress-intensity parameter, ΔK . The rate controlling process appears to be that associated with the creation of new crack surfaces in the range of crack growth rates 10^{-6} to 10^{-5} inch per cycle. The strong dependence of the apparent activation energy on ΔK suggests that a careful study of the kinetics of fatigue-crack growth and of the crack growth laws is in order. Such a study should incorporate both the mechanical and chemical variables involved.

9. F.J. Bradshaw and C. Wheeler 'The Effect of Environment on Fatigue-Crack Growth in Aluminum and Some Aluminum Alloys', Applied Materials Research, Vol. 5, 1966, pp. 112–120.

10. Waas, Anthony. (2018). Strength and Fatigue Testing of Composite Patches for Ship Plating Fracture Repair.

Explore and experimentally validate the use of composite patches for preventing crack growth and extending the lifetime of aluminum and steel ship structures. A composite patch works as a crack arrestor by decreasing the stress in the area of the crack tip. Load is shed from the base plate through an adhesive layer to the composite patch. In addition, the added constraint of the composite patch can prevent these cracks from coalescing into a larger crack. Analytical capabilities exist for predicting the effectiveness of the composite patch configuration, but such analyses demand specific idealizations and assumptions that must be validated experimentally in order for this technology to be used in practice. Our proposed project seeks to develop this technology as a useful and reliable tool for aluminum and steel ship plating fracture repair and to foster its industrial acceptance and implementation.

11. Phillips, E., An Experimental Study of Fatigue Crack Growth in Aluminum Sheet Subjected to Combined Bending and Membrane Stresses, NASA Technical Memorandum 4784, October 1997.

An experimental study was conducted to determine the effects of combined bending and membrane cyclic stresses on the fatigue crack growth behavior of aluminum sheet material. The materials used in the tests were 0.040-in.-thick 2024-T3 AL clad and 0.090-in.-thick 2024-T3 bare sheet. In the tests, the membrane stresses were applied as a constant amplitude loading at a stress ratio (minimum to maximum stress) of 0.02, and the bending stresses were applied as a constant amplitude deflection in phase with the membrane stresses. Tests were conducted at ratios of bending to membrane stresses

(B/7t4) of 0, 0.75, and 1.50. The general trends of the results were for larger effects of bending for the higher B/M ratios, the lower membrane stresses, and the thicker material. The addition of cyclic bending stresses to a test with cyclic membrane stresses had only a small effect on the growth rates of through-thickness cracks in the thin material, but had a significant effect on the crack growth rates of through-thickness cracks in the thick material. Adding bending stresses to a test had the most effect on the initiation and early growth of cracks and had less effect on the growth of long through-thickness cracks.

12. Leser, P. et. al., Mitigation of Crack Damage in Metallic Materials, NASA Technical Memorandum 218272, May 2014.

A system designed to mitigate or heal crack damage in metallic materials has been developed where the protected material or component is coated with a low-melting temperature film. After a crack is formed, the material is heated, melting the film which then infiltrates the crack opening through capillary action. Upon solidification, the healing material inhibits further crack damage in two ways. While the crack healing material is intact, it acts like an adhesive that bonds or bridges the crack faces together. After fatigue loading damages, the healing material in the crack mouth inhibits further crack growth by creating artificially high crack closure levels. Mechanical test data show that this method successfully arrests or retards crack growth in laboratory specimens.

13. Hedayati, E. and Vahedi, M., Using Extended Finite Element Method for Computation of the Stress Intensity Factor, Crack Growth Simulation and Predicting Fatigue Crack Growth in a Slant-Cracked Plate of 6061-T651 Aluminum, World Journal of Mechanics, Vol 4, No. 4, pp. 24-30, January 2014.

The 6061-T651 aluminum alloy is one of the most common aluminum alloys for marine components and general structures. The stress intensity factor (SIF) is an important parameter for estimating the life of the cracked structure. In this paper, the stress intensity factors of a slant-cracked plate, which is made of 6061-T651 aluminum, have been calculated using extended finite element method (XFEM) and finite element method (FEM) in ABAQUS software and the results were compared with theoretical values. Numerical values obtained from these two methods were close to the theoretical values. In simulations of crack growth at different crack angles, the crack propagation angle values were closer to the theoretical values in XFEM method. Also, the accuracy and validity of fatigue crack growth curve were much closer to the theoretical graph in XFEM than the FEM. Therefore, in this paper the capabilities of XFEM were realized in analyzing issues such as cracks.

14. Silling S. and Askari A., Peridynamic Model for Fatigue Cracking, Sandia Report SAND2014-18590, Sandia National Laboratories, Albuquerque, NM, 2014.

The peridynamic theory is an extension of traditional solid mechanics in which the field equations can be applied on discontinuities, such as growing cracks. This paper proposes

a bond damage model within peridynamics to treat the nucleation and growth of cracks due to cyclic loading. Bond damage occurs according to the evolution of a variable called the “remaining life” of each bond that changes over time according to the cyclic strain in the bond. It is shown that the model reproduces the main features of S-N data for typical materials and also reproduces the Paris law for fatigue crack growth. Extensions of the model account for the effects of loading spectrum, fatigue limit, and variable load ratio. A three-dimensional example illustrates the nucleation and growth of a helical fatigue crack in the torsion of an aluminum alloy rod.

15. Lua, J. et. al., XFEM Toolkit for Crack Path and Life Prediction of Aluminum Structures, Conference Paper – AIAA/ASME Structural dynamics and Materials Conference, May 2009.

This study is focused on the development and demonstration of the capability of the XFEM toolkit for ABAQUS (XFA) to predict fatigue crack growth and remaining life of 2D and 3D aluminum structures. The new technique couples the level set based crack description with the fast-marching method (FMM) for crack growth. Both the jump and tip enrichment functions are used to accurately capture the crack tip driving force during the fatigue crack growth prediction. To facilitate the crack insertion and definition within an existing FEM model without a crack, a customized ABAQUS CAE is developed to allow the user to specify the location, orientation, and size of the crack that is independent of the existing finite element mesh. Verification and validation studies are performed for the curvilinear crack growth and life prediction of 2D modified compact specimens and a 3D Weldment. The developed XFA package will allow the user to produce quantifiable metrics relating fatigue and fracture calculations to structural performance. In addition, the tool can be used to interpret the structural healthy monitoring data for risk informed decision making on repair, maintenance, and life extension options.

16. Donald, J.K. (2007), SR-1447 Fracture Mechanics Characterization of Aluminum Alloys for Marine Structural Applications.

High-performance aluminum ships also provide a number of operational challenges to the naval engineering community. First, the use of aluminum in the construction of the hull will lead to higher incidences of fatigue cracking; in addition, once fatigue cracks initiate, their growth in aluminum will be significantly greater than those in steel hulls. Other challenges associated with aluminum materials are stress-corrosion cracking and material sensitization during high operational temperatures.

17. Donald, J.K., Ship Structure Committee Report SSC-448, Fracture Mechanics Characterization of Aluminum Alloys for Marine Structural Applications, 2007.

The Ship Structure Committee (SSC) identified a lack of information required for structural integrity and damage tolerance analyses of aluminum marine structures. The development of such data is vital in light of the increased use of aluminum alloys in marine

construction. Under SSC project SR-1447, Fracture Technology Associates was contracted to characterize, through experimental fracture mechanics, the fatigue crack growth (FCG) resistance and fracture toughness of three aluminum alloys (5083, 5086, 5383) used in marine structural applications. Fatigue crack growth testing was performed following ASTM Standard E 647-00 in laboratory air at room temperature and in simulated ocean water per ASTM Standard D 1141. Non-linear fracture toughness testing was performed in accordance with ASTM Standard E 1820-01 in laboratory air at room temperature. For the three different grades of material, the difference in fatigue crack growth rate in laboratory air was negligible. In simulated seawater environment, AA5086 showed a slightly superior performance. In addition, all samples showed the same ranking of toughness with the 5086 showing the highest toughness, followed by 5083 and then 5383.

18. Makabe C, Naka K and Katsushima Y. Example of Arresting Crack Growth in Welded Parts, Industrial Engineering & Management 2015.

The unstable growth of fatigue cracks brings a material or structure to catastrophic failure. It is better than any fatigue crack does not initiate in engineering applications. However, fatigue crack initiation cannot be prevented in some applications because maintaining their efficiency or performance is important factor for usage. When a crack is initiated in machine equipment, it should be repaired, or the equipment replaced. Sometimes, the cracked material was repaired, and many repair methods were proposed. In this report, a simple method of stopping crack growth is proposed to apply to a cracked plate with varying thickness. The stop-hole and crack arrester were applied in the method presented in this publication.

19. Abaqus Software (version 6.14) documentation (Analysis User's Guide) by Dassault Systèmes Simulia Corp., section-11, Special-Purpose Techniques, subchapter-11.4 Fracture Mechanics.

Links:

https://link.springer.com/chapter/10.1007/978-1-4020-6239-1_1022
<http://www.dtic.mil/docs/citations/ADA025196>
<https://pdfs.semanticscholar.org/0789/f3e4f47cc65d5f7a117478b37419257e2b8b.pdf>
<https://www.sciencedirect.com/science/article/pii/S0093641399000646>
<https://www.sciencedirect.com/science/article/pii/S1350630707000519>
<http://www.etasr.com/index.php/ETASR/article/view/329/209>
<http://www.dtic.mil/dtic/tr/fulltext/u2/745989.pdf>
<https://link.springer.com/article/10.1007/BF001889439>
<https://www.researchgate.net/publication/254960594>
<https://ntrs.nasa.gov/archive/nasa/casi.ntrs.nasa.gov/19970034955.pdf>
<https://ntrs.nasa.gov/archive/nasa/casi.ntrs.nasa.gov/20140006911.pdf>
https://file.scirp.org/pdf/WJM_2014012017175092.pdf
<http://prod.sandia.gov/techlib/access-control.cgi/2014/1418590.pdf>
<https://www.researchgate.net/publication/268477400>
<https://www.researchgate.net/publication/277790664>
<http://www.shipstructure.org/pdf/448.pdf>

Sources:

Defense Technology Information Center (DTIC)
NASA Technical Reports Server (NTRS)
Google Scholar
Springer
Science Direct
Elsevier Scientific Ltd
Research Gate
US Naval Research Laboratory
Defense R&D Canada